

BOSTON UNIVERSITY

ME461: SENIOR DESIGN PROJECT

Rotor Design for Mars Exploration

Group Members:

Aidan Corrigan

Nathan Hepler

Tru Hoang

Kaustabh Singh

Capstone Advisor:

William Hauser

April 30, 2015

1 Abstract

Current efforts to explore Mars involve only two active rovers on the surface, Curiosity and Opportunity, and five active artificial satellites orbiting the planet. The Curiosity rover was designed to travel 200 meters per day while the Opportunity rover recorded a maximum range of 141 meters in a day in 2004. To expand the coverage range, scientists and engineers at NASA are developing unmanned aerial vehicles (UAV) equipped with sensors to provide the next generation of rovers with a topographical image of Martian terrain for path-planning purposes. This team proposed a design of the rotor mechanism for a Mars rotorcraft.

In developing the mechanism, a mathematical model of a coaxial rotor configuration was created to estimate its performance parameters. A scaled prototype was manufactured and assembled for testing. The test results were compared to the theoretical calculations.

Contents

1	Abstract	1
2	Background	7
3	Benchmarking	7
4	Acknowledgements	9
5	Design Objectives	10
6	Requirements	10
7	Engineering Specifications	11
7.1	Atmospheric Specifications	11
7.2	Rotorcraft Specifications	12
8	Design Process	12
8.1	System Architecture	12
8.2	Functional Decomposition	13
8.3	Concept Selection	14
9	Theory	17
9.1	Conventional Helicopter Rotor	18
9.2	Coaxial Rotor	19
9.3	Theoretical Results	21
9.4	Detailed Final Design	22
9.5	Prototype Design	24
10	Testing and Results	25
11	Multiple Success Points	29
12	Space Grading	29

13 Financial Considerations	31
Appendices	33
Appendix A Calculations	33
Appendix B Scaling	36
Appendix C Testing Calculations	38
Appendix D Gantt Charts	40
Appendix E Space Grading	42
Appendix F Scaled Design Drawings	43
Appendix G Ordered Part Specifications	55
Appendix H Manufacturing Procedure	64
Appendix I MATLAB Code	66

List of Figures

1	NASA Martian Rotorcraft Concept	8
2	Detailed Design of MARV Rotorcraft	8
3	Velocity Profile of Rotor Mechanism from Ground to Hover	11
4	System Architecture of our project.	13
5	Functional Decomposition of the rotor mechanism.	13
6	Theory Flow Chart	17
7	Flow model of a coaxial rotor system with the lower rotor operating in the fully developed slipstream of the upper rotor.[2]	20
8	Left: Isometric view of gearbox. Right: Section view of gearbox.	23
9	Render of the rotor mechanism in a Martian environment.	23
10	Isometric view of final design.	24
11	Current as a function of voltage for a no-load motor test.	25
12	Beam Testing Apparatus	26
13	No-Beam Testing Apparatus	26
14	Lift generated as a function of input motor torque.	27
15	Motor RPM as a function of motor torque.	28
16	Lift generated as a function of input motor torque.	28
17	Breakdown of Final Mission Costs	32
18	Free Body Diagram of the forces acting on the rover during climb.	34
19	The induced velocity as a function of radius for the upper and lower propellers.	35
20	Reynolds Number and Mach number as a function of radius along the blade.	35
21	Detailed Gantt chart of project.	40
22	Abbreviated Gantt chart of project.	41
23	Radiation comparison between Earth and Mars.	42
24	Schematic Drawing of the Base Plate.	43
25	Schematic Drawing of a Bottom of the Gear Box.	44
26	Schematic Drawing of a Side of the Gear Box.	45
27	Schematic Drawing of a Side of the Gear Box.	46

28	Schematic Drawing of a Side of the Gear Box.	47
29	Schematic Drawing of the Top of the Gear Box.	48
30	Schematic Drawing of the Motor Mount.	49
31	Schematic Drawing of the Drive Shaft.	50
32	Schematic Drawing of the Inner Shaft.	51
33	Schematic Drawing of the Outer Shaft.	52
34	Schematic Drawing of an Airfoil.	53
35	Schematic Drawing of an Airfoil.	54
36	Aluminum Rod Specifications.	55
37	Bevel Gear Specifications.	56
38	Large Ball Bearing Specifications.	57
39	Small Ball Bearing Specifications.	58
40	Coupling Spider Specifications.	59
41	Coupling Hub Specifications.	60
42	Large Retaining Ring Specifications.	61
43	Small Retaining Ring Specifications.	62
44	Motor Specifications.	63

List of Tables

1	Atmospheric Comparison between Mars and Earth	12
2	Preliminary Morphological Chart	14
3	Pugh Chart for Generating Lift	15
4	Pugh Chart for Balancing Torque	15
5	Pugh Chart for Generating Torque	16
6	Pugh Chart for Transmitting Torque	16
7	Final Morphological Chart	16
8	Final Design Performance Summary	22
9	Scaled Design Performance Summary	24
10	Cost Summary	31
11	Summary of parameters used in calculations	33

2 Background

Gathering data from the Martian surface is limited by the speed and scope of Mars rovers. There are currently two operational rovers on Mars: Opportunity and Curiosity. Opportunity landed on Mars on January 25th, 2004 and has traveled 42 kilometers since its arrival. Curiosity currently traverses the Martian landscape at a rate of 400 meters per month. NASA is currently planning another rover mission to Mars in 2020 in which the rover will house a small helicopter drone.¹ Although the rovers are successful in collecting large amounts of scientific data, their methods of doing so are slow. To increase the rate of data collection, the use of rotorcraft has been proposed for scouting ahead of rovers and for carrying scientific payloads. The difficulty of this mission lies in the composition of the Martian atmosphere. Traditional methods of determining the rotorcraft's performance need to be altered to account for a nearly 100% decrease in atmospheric density and a 70% reduction in gravity (compared to Earth). The Mars rotorcraft field is relatively unexplored and a functioning vehicle has yet to be completed.

3 Benchmarking

This project builds on the endeavors of two groups in the aerospace field: the NASA Jet Propulsion Laboratory (JPL) and the University of Maryland. Researchers at JPL are working on a prototype coaxial rotorcraft that has the capability to fly 0.5 km every day for about 2 to 3 minutes. It has a mass of 1 kg and a blade radius of 0.55 m. Currently, the prototype is undergoing extensive testing for approval to be launched with NASA's next rover mission. The NASA prototype is shown in Figure 1².

¹"Helicopter Could Be 'Scout' for Mars Rovers", <http://www.nasa.gov/jpl/helicopter-could-be-scout-for-mars-rovers>

²NASA Mars Helicopter Prototype, <http://www.jpl.nasa.gov/news/news.php?feature=4457>.



Figure 1: NASA Martian Rotorcraft Concept

Students at the University of Maryland proposed the preliminary design of the coaxial Martian Autonomous Rotary Wing Vehicle (MARV). MARV has a gross mass of 50 kilograms, a blade radius of 2.1 meters and a flight range of 25 kilometers with a maximum altitude of 100 meters. The MARV prototype is shown in Figure 2[1].

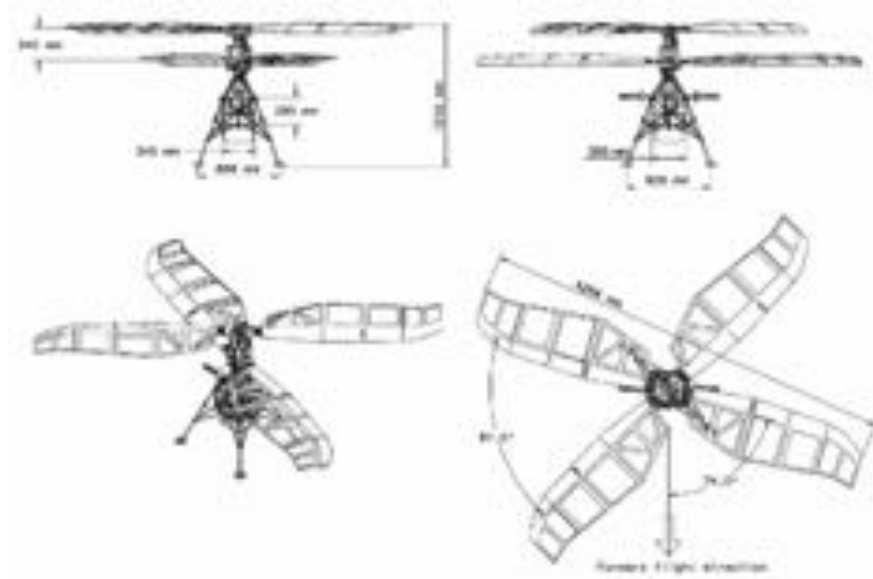


Figure 2: Detailed Design of MARV Rotorcraft

4 Acknowledgements

- **Larry Young** - *Primary Consultant*

NASA Ames Research Center, Army/NASA Rotorcraft Division

Larry worked on a similar project involving Mars rotorcraft at NASA Ames. He has provided us with the means of making necessary calculations via Excel spreadsheets and he has showed us many research papers that this project is based off of.

- **Richard Otero, PhD** - *Consultant*

EDL Systems and Advanced Technologies Group

Dr. Otero was our initial consultant and helped us with getting our project started.

- **William Hauser, PhD** - *Capstone Advisor*

Boston University Mechanical Engineering Department

Professor Hauser has met with us weekly and provided constant feedback and guidance throughout the project.

- **Ray Nagem, PhD** - *ME Consultant*

Boston University Mechanical Engineering Department

Professor Nagem has helped us with the mechanics of the rotor design and calculations regarding the Martian atmosphere.

- **James Geiger, MS** - *Aircraft Consultant*

Boston University

Professor Geiger has extensive experience in rotor design at GE and has helped us set realistic goals for our project as well as providing feedback for the completed work thus far.

- **Ryan Lacy** - *Machining Consultant*

Boston University

- **Joe Estano, MS** - *Machining Consultant*

Boston University

5 Design Objectives

The goal of this project is to propose a preliminary design of a rotor mechanism for a rotorcraft that can achieve vertical translation on Mars. The specific objectives that need to be met to complete this goal are:

- Learn basic helicopter aerodynamics
- Model a rotor mechanism to generate lift in the Martian environment
- Perform scaling analysis to enable testing within available facilities
- Test resulting scaled model
- Compare test results to theoretical calculations

6 Requirements

To enable a design study for this mechanism, we established the following as nominal requirements:

1. Total Mass: 5 kilograms
2. Ascension Time: 20 seconds
3. Ascension Distance: 10 meters

The rotor mechanism will be fitted for a rotorcraft with a total mass of 5 kilograms. An altitude of 10 meters was determined to be sufficient for a panoramic view of the terrain. An ascension time of 20 seconds, including a combined acceleration and deceleration time of 3.2 seconds, was chosen to reduce the required motor torque. The ascension velocity profile is shown in Figure 3. This yields a maximum climb velocity of 0.556 m/s with an acceleration of 0.348 m/s^2 from 0 to 1.6 seconds and a deceleration of equal magnitude from 18.4 to 20 seconds. Although the analysis on this velocity curve is an important step in the design process, the lift required to climb only accounts for 8% of the total lift while the other 92% comes from achieving hover.

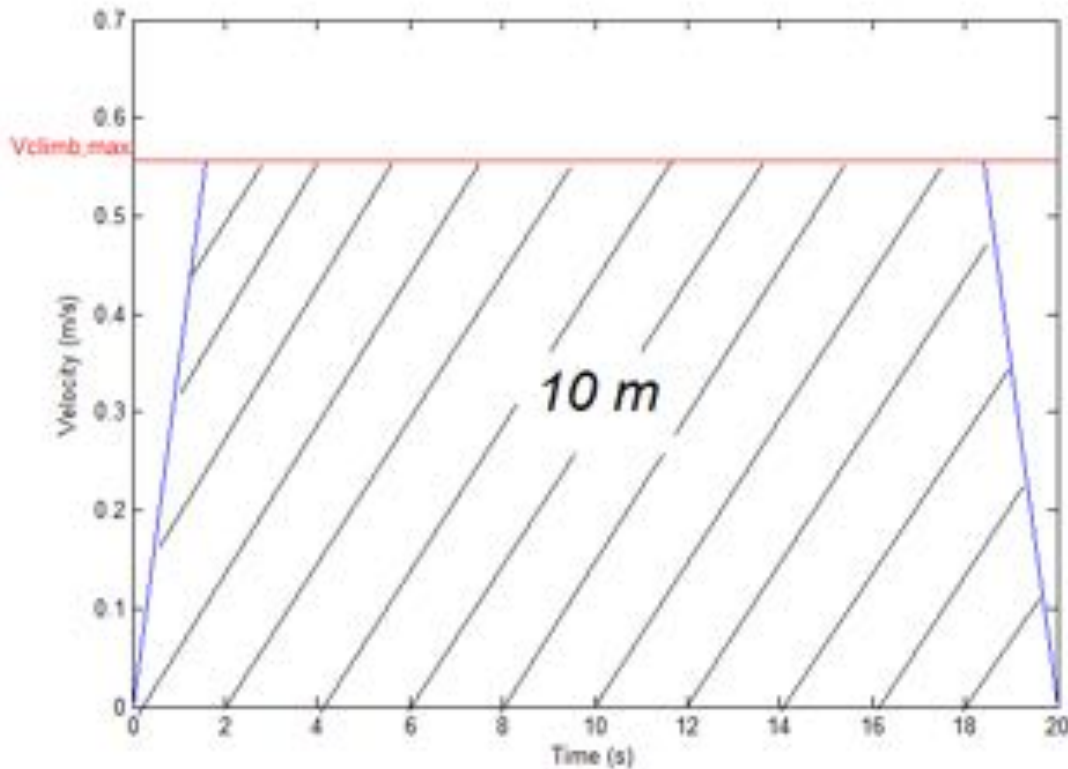


Figure 3: Velocity Profile of Rotor Mechanism from Ground to Hover

7 Engineering Specifications

7.1 Atmospheric Specifications

An important factor governing the design of the rotor mechanism is the difference between the atmospheric densities of Earth and Mars. The lower atmospheric density of Mars limits the ability of an aerial vehicle to generate lift because the general lift expression is directly proportional to the density of a fluid. Flying through the Martian atmosphere near the planet's surface is comparable to flying at about 12,000 meters (40,000 feet) on Earth. The adiabatic coefficient of CO_2 ($\gamma = 1.3$) was used to calculate the speed of sound ($a = \sqrt{\gamma P / \rho}$) because the atmospheric composition of Mars is 95% CO_2 ³. The relevant parameters are listed in Table 1.

³<http://nssdc.gsfc.nasa.gov/planetary/factsheet/marsfact.html>

Table 1: Atmospheric Comparison between Mars and Earth

Specification	Mars Value	Earth Value
g (m/s ²)	3.711	9.81
ρ (kg/m ³)	0.0155	1.217
P (Pa)	636	101350
Average T (K)	210	288
a (speed of sound) (m/s)	227	343
CO ₂ Content (%)	95.32	0.04

7.2 Rotorcraft Specifications

To begin the design process, we specified physical constraints based on similar projects [1][3]. The tip speed of the propellers was limited by a Mach number of 0.65[3]. This is a conventional value that is used for rotor design. The calculations for the required thrust can be found in Appendix A.

- Blade Tip Mach Number: 0.65
- Required Thrust: 20.3 N

8 Design Process

8.1 System Architecture

The System Architecture in Figure 4 depicts the various components of the rotor mechanism that needed to be designed. The mechanism consists of two primary categories: the propellers and the power train. The propellers are characterized by several properties, which includes the radius, chord length, airfoil selection, angle-of-attack, and blade twist. Determining these properties required modeling of the aerodynamics to verify that the selections would satisfy the required thrust to achieve lift. The power train (composed of the gear train, shafts, and the motor) had to be developed based on the transmission and required torque of the system.

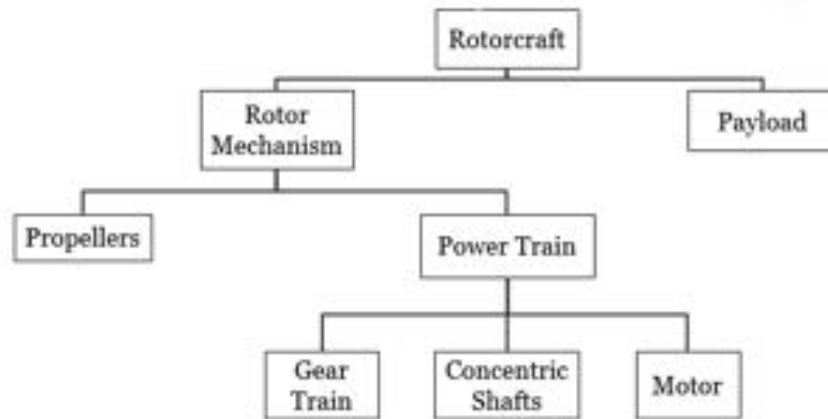


Figure 4: System Architecture of our project.

8.2 Functional Decomposition

The essential goal of the rotor mechanism is to follow the velocity profile defined in Figure 3. In order to do so, four functions must be achieved to meet the requirements. These functions are outlined in Figure 5.

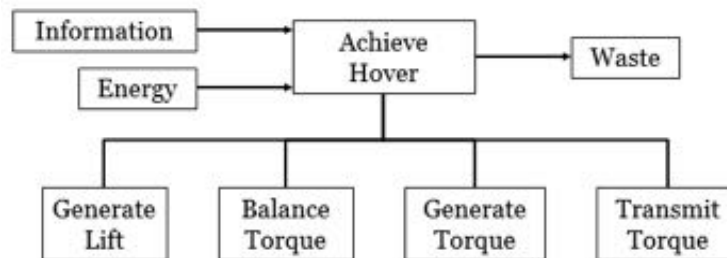


Figure 5: Functional Decomposition of the rotor mechanism.

First and foremost, the rotor mechanism needs to be able to generate lift to depart from the ground. Since this project covers the design of a mechanism for a rotary-wing vehicle, there are really only two candidates for this function: a propeller and a rotor. The selection between the two is covered in the next section.

Since the design of a rotorcraft incorporates many rotating components, particularly the rotary disks, the overall torque of the system must be balanced. If this function is not met, the rotorcraft will be unstable.

In order to power the entire mechanism, an adequate torque generator must be

chosen. Such a generator would be in the form of a motor or engine and would need to be able to provide sufficient torque.

Lastly, there needs to be a method to transmit the torque from the generator to the rotors. This would likely include the use of a gearbox to change the direction and possibly magnitude of the generated torque.

8.3 Concept Selection

The final design components were selected using a combination of Morphological and Pugh charts as shown in Tables 2 through 6 with the final design selection shown in Table 7.

Table 2: Preliminary Morphological Chart

Function	1	2	3	4
Lift	Propeller ⁴ 	Rotor ⁵ 	—	—
Balance Torque	Quadrotor ⁶ 	Coaxial ⁷ 	Conventional ⁸ 	Tandem ⁹ 
Generate Torque	DC Brushed Motor	DC Brushless Motor	AC Motor	—
Transmit Torque	Single-Motor	Multi-Motor	—	—

The driving factor of generating lift was the simplicity of design. The difference between a rotor and a propeller is that a propeller is fixed-pitch along the entirety of the blade length while the rotor has control systems capable of changing the angle-of-attack mid-flight. These changes are accomplished through the means of feathering, lagging, and flapping, each

⁴GWS 3-Blade Propeller, <http://multicoptersystems.com/multicoptersystems-com-waltzmart-gws-ep-5030-5x3-3-blade-propeller-cw-props-multi-rotor-quad-copter-pack-of-2-from-multicoptersystems-com/>.

⁵Rotor, <http://www.walkeraside.com/what-is-blade-tracking.htm>.

⁶JAviator Top View, <http://javiator.cs.uni-salzburg.at/releases/javiator-v2-advanced-blueprints/index.html>.

⁷VIKI Coaxial Helicopter, <http://www.rotaryforum.com/forum/showthread.php?t=10464&page=7>.

⁸Tail Rotor, <http://www.smallhelis.com/intro-to-rc-helis/coaxial-vs-conventional/>.

⁹V-50 Tandem-Rotor Helicopter, <http://www.aviastar.org/helicopters-eng/kamov=v-50.php>.

of which requires its own mechanism (a swashplate) to operate. Incorporating these means of control is complicated and unnecessary for achieving vertical lift of a rotorcraft. Therefore, a propeller was selected for use (*propeller* and *rotor* will be used interchangeably throughout the report).

Table 3: Pugh Chart for Generating Lift

Requirements	Weight	Propeller	Rotor
Simplicity of Design	2	0	-1
Cost	1	0	-1
Manufacturability	1	0	1
Ease of assembly	1	0	-1
Total		0	-3

Stability and compactness have the most influence over the torque balancing of the vehicle. Due to the presence of a single, large rotor that spins in one direction, conventional helicopters are inherently unstable. Rotorcraft with quadrotor, coaxial, or tandem configurations all have multiple rotors that counter-rotate; as such, they can all achieve the same level of stability. Since coaxial rotorcraft have their rotor planes aligned on top of each other, it is more compact than the other configurations. This reduces the complexity of transportation to Mars.

Table 4: Pugh Chart for Balancing Torque

Requirements	Weight	Quadrotor	Coaxial	Conventional	Tandem (front rear)
Stability	2	0	0	-1	0
Compactness	2	0	1	-1	-1
Maneuverability	1	0	0	-1	-1
Total		0	2	-5	-3

It is easier to vary the revolutions per minute (RPM) of a DC motor because the RPM is directly proportional to the input voltage, whereas an AC motor only accepts a sinusoidal input. A function generator can be used to control an AC motor while a simple

DC power supply can directly control a DC motor. A DC brushless motor requires a specific controller to vary the RPM, making it undesirable.

Table 5: Pugh Chart for Generating Torque

Requirements	Weight	DC Brushed Motor	DC Brushless Motor	AC Motor
Cost	1	0	-1	-1
RPM Variability	2	0	0	-1
Controllability	2	0	-1	0
Total		0	-3	-3

A one motor system is cheaper compared to a multiple-motor system. Additional motors can also put extra weight on the already weight-constricted structure.

Table 6: Pugh Chart for Transmitting Torque

Requirements	Weight	Single Motor	Multi-Motor Transmission Train
Simplicity of Design	1	0	0
Cost	2	0	-1
Gross Weight	1	0	-1
Total		0	-1

Table 7: Final Morphological Chart

Function	1	2	3	4
Lift	Propeller	Rotor	—	—
Torque Balance Configuration	Quadrotor	Coaxial	Conventional	Tandem
Torque Generator	DC Brushed Motor	DC Brushless Motor	AC Motor	—
Torque Transmission	Single-Motor	Multi-Motor	—	—

9 Theory

The derivation of a mathematical model for a coaxial rotor system first required a basic understanding of a conventional helicopter configuration. Modifying this understanding to account for the effects of the upper rotor on the lower rotor, we used the derived equations and varied the physical parameters to match the required thrust listed in Section 7.2. Once the thrust and physical dimensions were determined, we were able to calculate the power and torque required to generate said thrust. A flow chart of this iterative process is shown in Figure 6.

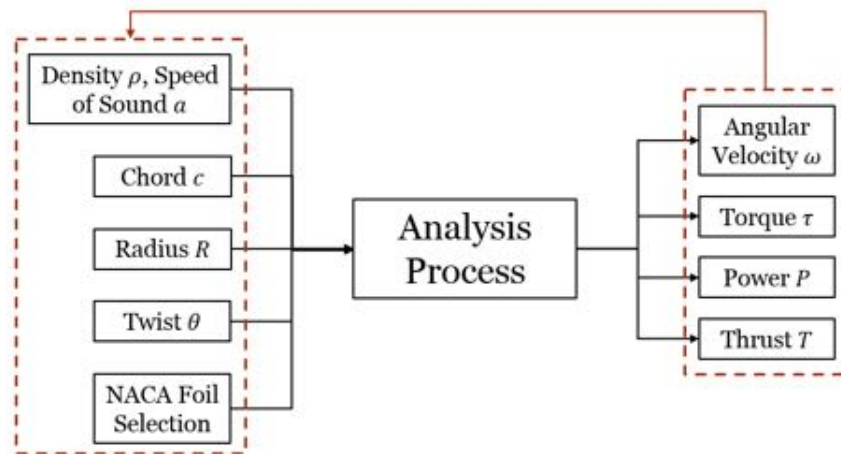


Figure 6: Theory Flow Chart

9.1 Conventional Helicopter Rotor

The helicopter rotor produces an upward thrust by driving a column of air downwards through the rotor plane. Applying Newtonian mechanics - the laws of conservation of mass, momentum, and energy - to the analysis of this process allows us to establish a relationship between the thrust produced and the velocity communicated to the air. This approach is referred to as the momentum theory for helicopters and the rotor is considered an "actuator disc". It can be shown that the thrust and the power in hover are given by

$$T = 2\rho A v_i^2 \quad (1)$$

$$P = \frac{T^{\frac{3}{2}}}{\sqrt{2\rho A}} \quad (2)$$

where T is the thrust, ρ is the air density, A is the disc area, and v_i is the induced velocity.

Similarly, the thrust and power in vertical flight are given by:

$$T = 2\rho A (V_c + v_i) v_i \quad (3)$$

$$P = T(V_c + v_i) \quad (4)$$

where V_c is the rate of climb of the rotor.

For convenience, these variables were non-dimensionalized. Then we have, for coefficients of thrust, power, and velocity:

$$C_T = \frac{T}{\rho A (\Omega R)^2} \quad (5)$$

$$C_P = \frac{P}{\rho A (\Omega R)^3} \quad (6)$$

$$\lambda_i = \frac{v_i}{\Omega R} \quad (7)$$

Here, ΩR is the rotor tip speed, where Ω is the angular velocity and R is the propeller radius. λ is often referred to as the non-dimensionalized inflow velocity.

Equations 1 through 7 provide the designers with the tools to calculate the desired performance of the vehicle. However, they do not include the effect of the blades' shape and dimensions. Thus, a more comprehensive analysis is required.

Blade element momentum theory (BEMT) applies the standard process of airfoil theory to the rotating blade. This method allows the designer to vary the design parameters of the

rotor blades to achieve the thrust and power calculated using the simple momentum theory. For simplicity, only the relevant equations to our project are listed. The derivations can be found in [2].

$$\alpha = \theta - \phi \quad (8)$$

$$\lambda = r\phi \quad (9)$$

$$dC_T = 4\lambda^2 r dr \quad (10)$$

$$dC_Q = \frac{1}{2}\sigma(\lambda C_L r^2 + C_D r^3) dr \quad (11)$$

$$P = \Omega Q \quad (12)$$

In Equation 8, α is the angle-of-attack, θ is the pitch angle or twist angle, and ϕ is the inflow angle. The coefficient of blade torque is represented by C_Q and is related to the rotor power by Equation 12. The solidity factor, σ , is given by $\sigma = Nc/\pi R$, where N is the number of blades and c is the chord length.. The lift coefficient C_L can be approximated by the linear Equation $C_L = a(\theta - \phi)$ where a is the lift slope factor. r is the non-dimensionalized radius of the rotor disc.

A new expression for the non-uniform inflow velocity as a function of the rotor radius is:

$$\lambda(r) = \frac{\sigma a}{16} \sqrt{\left(1 + \frac{32}{\sigma a} \theta r\right) - 1} \quad (13)$$

This expression was important because it relates the dimensions of the propeller blades to the thrust and torque coefficients shown in Equations 10 and 11. These methods were used to derive a new expression for the non-dimensionalized inflow velocity for each propeller in a coaxial system.

9.2 Coaxial Rotor

In [2], Leishman and Ananthan applied momentum theory and BEMT in their analysis of the coaxial rotor and derived new equations that take into account the effects of the upper rotor on the lower rotor. Here, their research is summarized and the new equations for the inflow velocity, thrust coefficient, and power coefficient are listed.

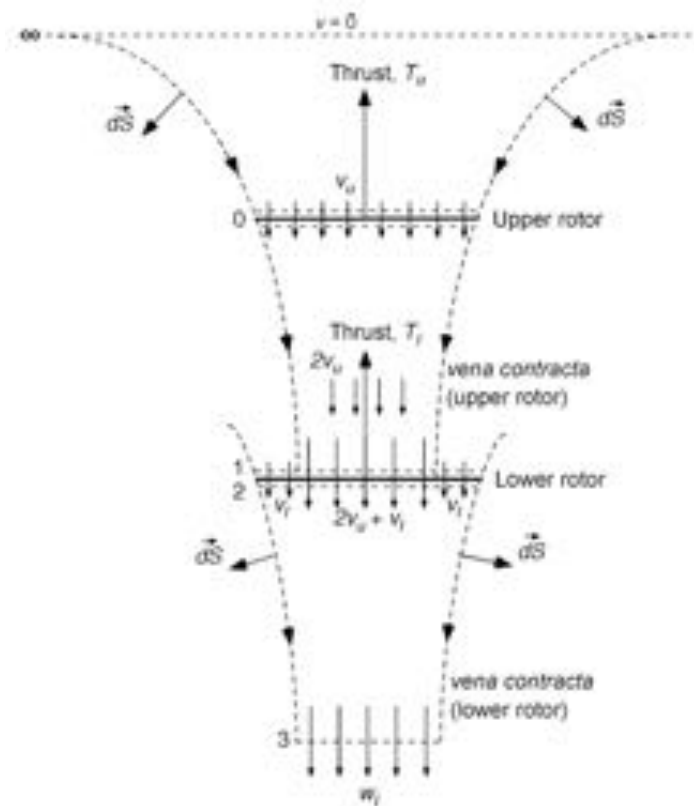


Figure 7: Flow model of a coaxial rotor system with the lower rotor operating in the fully developed slipstream of the upper rotor.[2]

Figure 7 shows the model that was used for the analysis. It is to be noted that this model assumes both rotors operate at an equal balanced torque.

The BEMT analysis of the equal balanced torque model yields the following equations:

$$\lambda_u(r, \lambda_\infty) = \sqrt{\left(\frac{\sigma C_{l_\alpha}}{16F} - \frac{\lambda_\infty}{2}\right)^2 + \frac{\sigma C_{l_\alpha}}{8F} \theta_u r} - \left(\frac{\sigma C_{l_\alpha}}{16F} - \frac{\lambda_\infty}{2}\right) \quad (14)$$

$$\begin{aligned} \lambda_l(r \leq r_c, \lambda_\infty) &= \sqrt{\left(\frac{\sigma C_{l_\alpha}}{16F} - \frac{\lambda_\infty + (A/A_c)\lambda_u}{2}\right)^2 + \frac{\sigma C_{l_\alpha}}{8F} \theta_u r} \\ &- \left(\frac{\sigma C_{l_\alpha}}{16F} - \frac{\lambda_\infty + (A/A_c)\lambda_u}{2}\right) \end{aligned} \quad (15)$$

$$\lambda_l(r > r_c, \lambda_\infty) = \sqrt{\left(\frac{\sigma C_{l_\alpha}}{16F} - \frac{\lambda_\infty}{2}\right)^2 + \frac{\sigma C_{l_\alpha}}{8F} \theta_u r} - \left(\frac{\sigma C_{l_\alpha}}{16F} - \frac{\lambda_\infty}{2}\right) \quad (16)$$

$$C_T = 4 \int_0^1 \lambda_u^2 r dr \quad (17)$$

$$C_P = 4 \int_0^1 \lambda_u^3 r dr \quad (18)$$

where λ_u is the inflow velocity of the upper rotor, λ_l is the inflow velocity of the lower rotor, λ_∞ is the climb velocity, C_{l_α} is the lift-curve slope of the airfoil, F is the Prandtl tip-loss factor, A is the rotor disc area, A_c is the contracted wake area, and r_c is the radial contraction of the wake seen in Figure 7.

Leishman and Ananthan termed the fully developed slipstream of the upper rotor the *vena contracta*. The flow velocity of the lower rotor in this region is different than that of the unaffected region. This is reflected in Equations 15 and 16. Equations 17 and 18 can be plugged into Equations 5 and 6 to give us values for thrust and power. The results are shown in Appendix A.

9.3 Theoretical Results

The driving input parameters that determine the produced thrust are the radius, chord length, and twist. An increase in radius and chord resulted in an increase in generated thrust but also increased the required torque and therefore, a larger motor. The process was optimized via MATLAB code (Appendix I). We minimized the radius by changing the chord and twist to match the required lift from the Rotorcraft Specifications. While analyzing Equation 6, it is clear that more power is required on Earth compared to Mars due to the direct correlation with atmospheric density. Equation 13 was analyzed to compare the lift

generation between coaxial and conventional helicopters. With the same inputs, a coaxial helicopter produces approximately four times more thrust than a conventional helicopter.

9.4 Detailed Final Design

The iterative process for theoretical calculations yielded the following final propeller design parameters:

$R = 1.5 \text{ m}$
$c = 0.30 \text{ m}$
$\theta = 30^\circ$

We selected the NACA 23012 airfoil for the propellers, which is a standard rotorcraft airfoil. These characteristics resulted in the performance parameters shown in Table 8. There are two stages of the vertical flight phase that we are designing around: climb and hover. 90% of the required lift is accounted for by hovering. For hover, the thrust equal to the weight and for climb there is another force accelerating the rotorcraft upwards. The required values for lift are:

$$\text{Hover Lift} = 18.5 \text{ N}$$

$$\text{Climb Lift} = 20.3 \text{ N}$$

The results of the analysis indicated with given R , c , and θ are:

Table 8: Final Design Performance Summary

Parameter	Hover	Climb	Units
Thrust	20.8	31.3	N
Power	129	227	W
Torque	1.29	2.27	N·m

To achieve the coaxial balanced torque configuration we selected a differential gear train to evenly distribute the motor torque to each of propeller shafts. The section view of the gearbox (Figure 8) shows the counter-rotating concentric shafts which are connected to the gear train using retaining rings and set screws. Appropriately sized bearings were fitted

between the rotating shafts and the gearbox housing to reduce frictional losses. Figures 9 and 10 show the CAD for the final design¹⁰

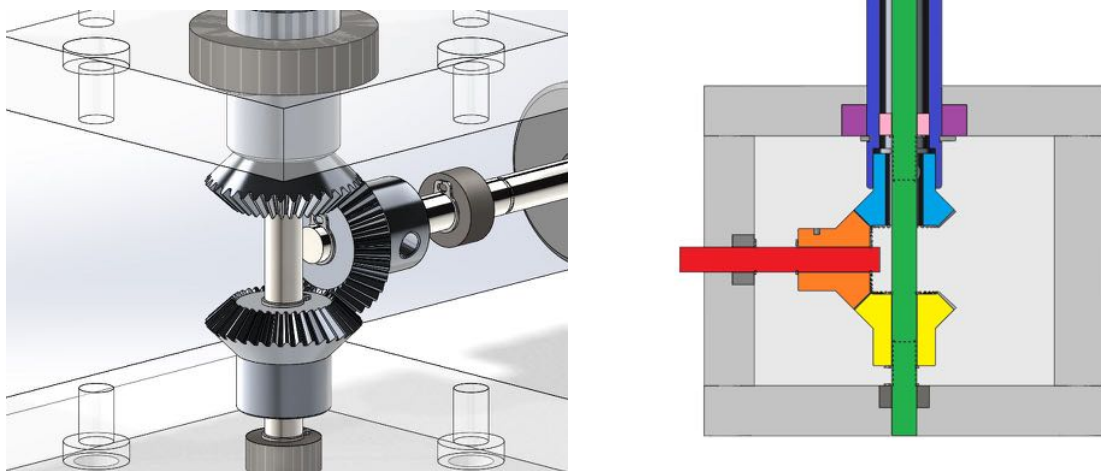


Figure 8: Left: Isometric view of gearbox. Right: Section view of gearbox.

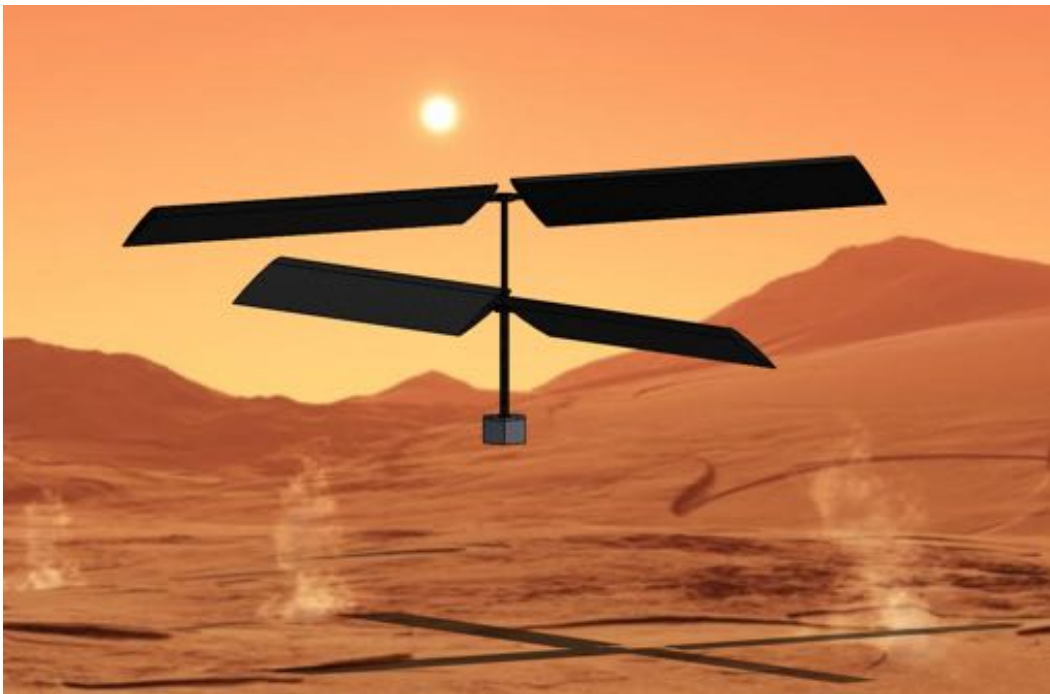


Figure 9: Render of the rotor mechanism in a Martian environment.

¹⁰<http://www.redorbit.com/news/space/1113024596/mars-surface-radiation-almost-suitable-for-manned-mission-121013/>



Figure 10: Isometric view of final design.

9.5 Prototype Design

The Buckingham Pi Theorem was used to scale our final design that would operate on Mars to a prototype that we could test on Earth, based on the thrust, power, and torque as seen in Table 9. These calculations are shown in Appendix B. Our restrictions for the scaling procedure were to maintain a constant Reynold's Number and a constant c/R ratio.

Table 9: Scaled Design Performance Summary

Parameter	Hover	Climb	Units
Thrust	0.484	0.759	N
Power	0.547	0.964	W
Torque	0.031	0.055	N·m

Appendix F shows detailed drawings of the scaled design. The machining of the prototype proved to be difficult in that the accuracy of the parts had to be within $\pm 0.0005''$. Several parts did not dimensionally match with specs provided by the manufacturer, so last minute alterations to the CAD and drawings had to be made to account for said errors.

10 Testing and Results

Figure 11 shows the no-load motor test results. The motor was connected directly up to a DC power supply and the voltage was varied from 0 to 6 volts. A linear trend was applied (excluding outliers) to achieve an equation relating the input voltage to the current drawn.

There were two types of testing performed, one with a balance beam and one without.

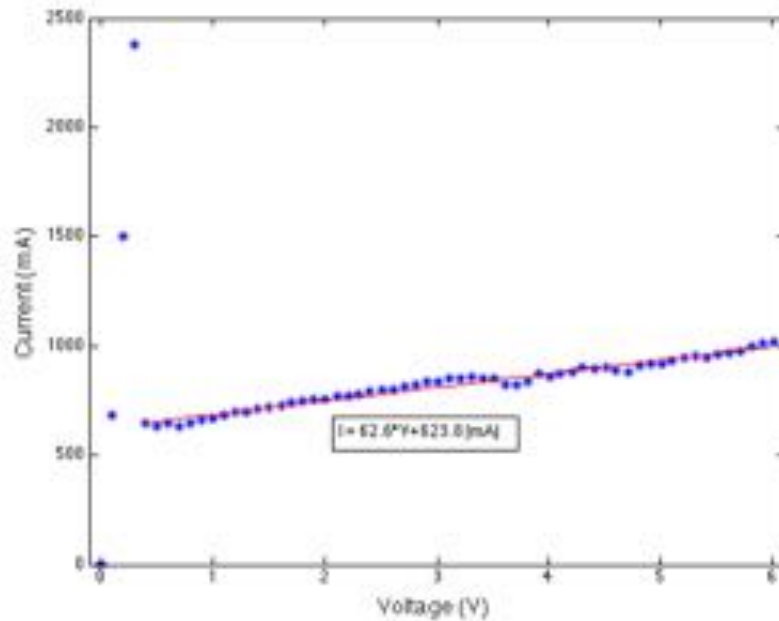


Figure 11: Current as a function of voltage for a no-load motor test.

The balance beam testing apparatus is shown in Figure 12. The beam is balanced with one side on top of a scale and the other side screwed to the rotor mechanism. When the mechanism generates lift, the beam will depress the scale with a reducing ratio of 0.38, determined by the relative arm lengths of the beam. The other testing configuration consists of the rotor mechanism fixed to the top of the scale. The no-beam testing configuration is shown in Figure 13.

These two test methods were performed to compare the significance of the ground effect. The ground effect increases lift when the vehicle is close to the ground; therefore, misrepresenting the lift generated at higher altitudes. The beam test reduced the area under the rotors which causes the ground effect.

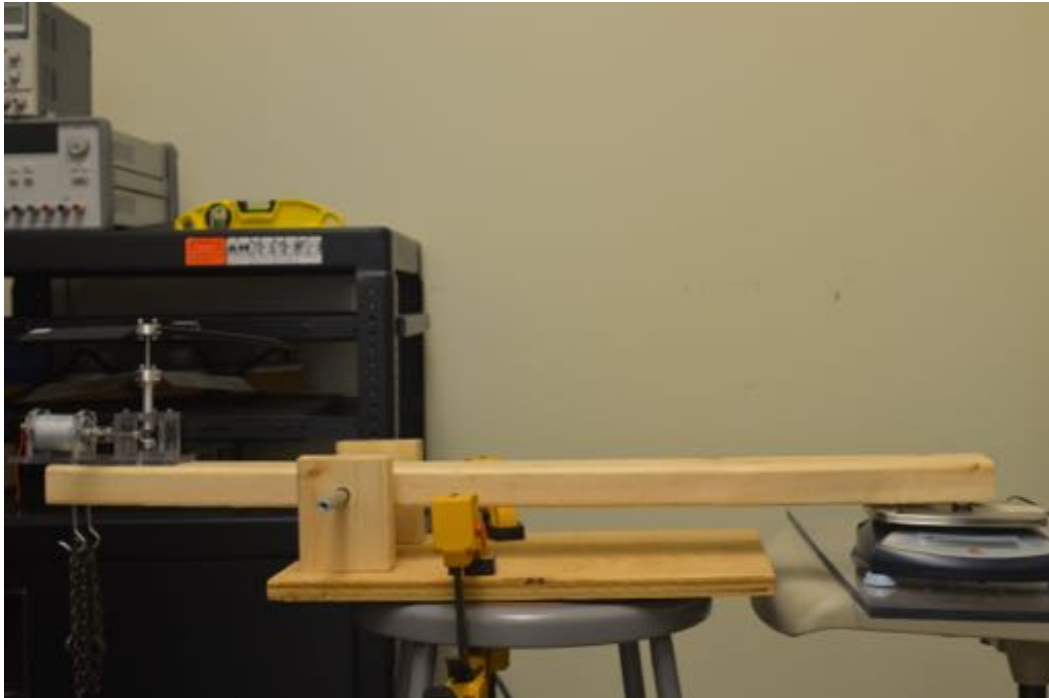


Figure 12: Beam Testing Apparatus

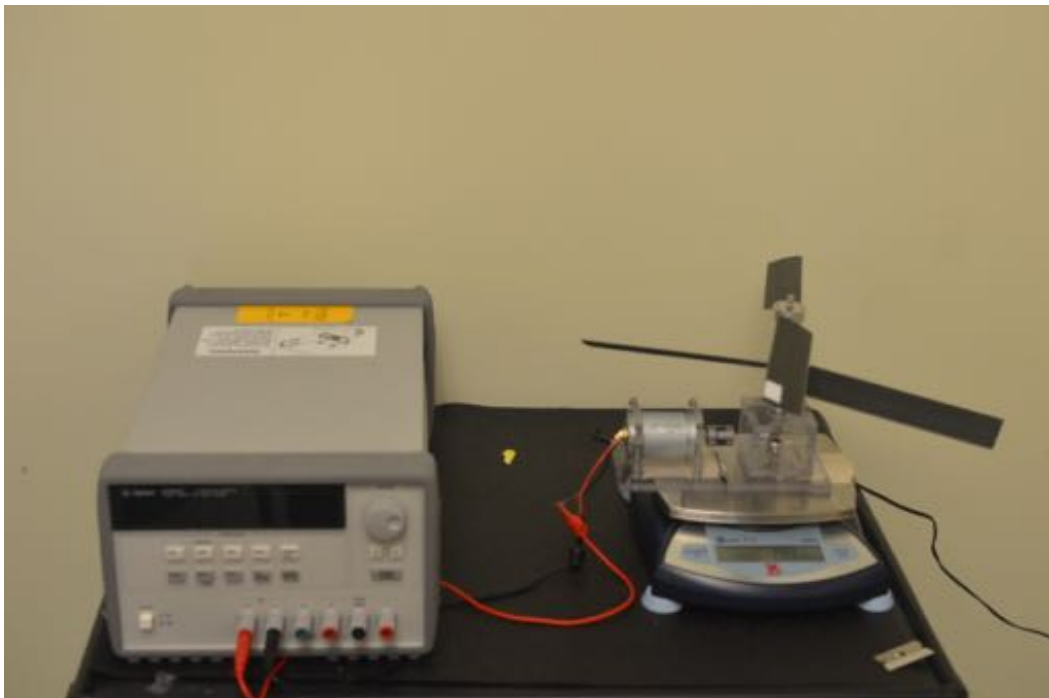


Figure 13: No-Beam Testing Apparatus .

The tests included a voltage sweep using a DC power supply to measure the lift, RPM, and current at each measurement unit. Two different power supplies were used: an Agilent DC power supply was used to supply up to 5 amps because it has an upper current limit of 5 amps and a TekPower DC power supply was used to supply current from 5 to 10 amps. The Agilent power supply was used for the first half of the measurements because it has a higher resolution than the TekPower supply.

To confirm our theoretical calculations, a lift of 0.484 newtons had to be achieved at a torque of 0.0352 newton-meters. The lift and torque values are equivalent to a digital scale reading of 49.4 grams and a supplied current of 6.01 amps, respectively. Figures 14 and 15 show the generated lift and the RPM of the mechanism as a function of motor torque for each testing configuration.

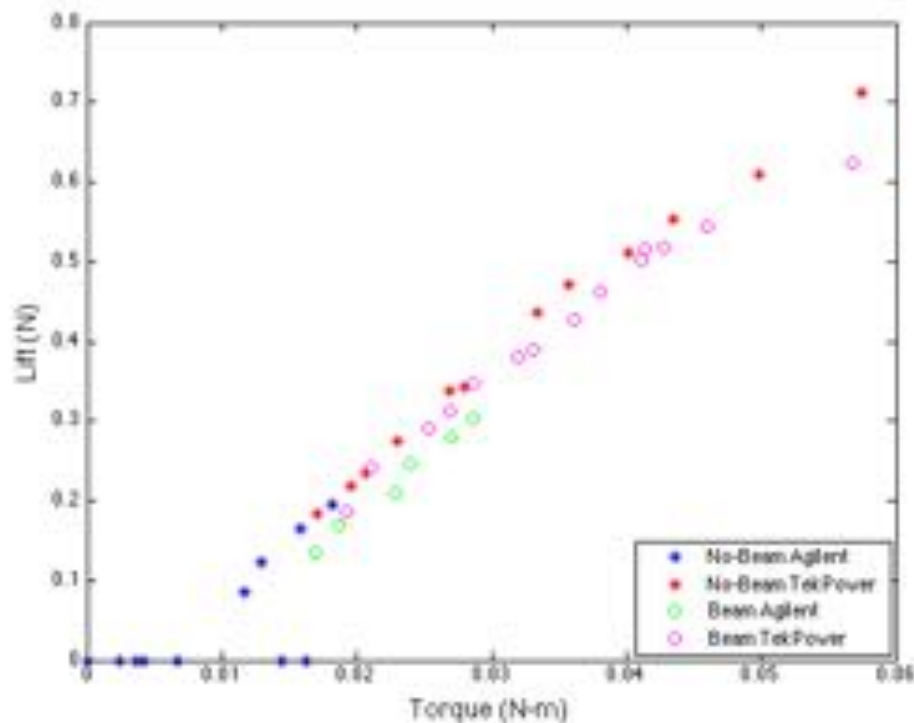


Figure 14: Lift generated as a function of input motor torque.

Figure 16 shows the no-beam test with the TekPower Power Supply. The data point that needed to be achieved was 0.484 newtons at 0.0352 newton-meters. We measured a lift of 0.471 newtons at a torque of 0.3575 newton-meters which is very close to the desired value.

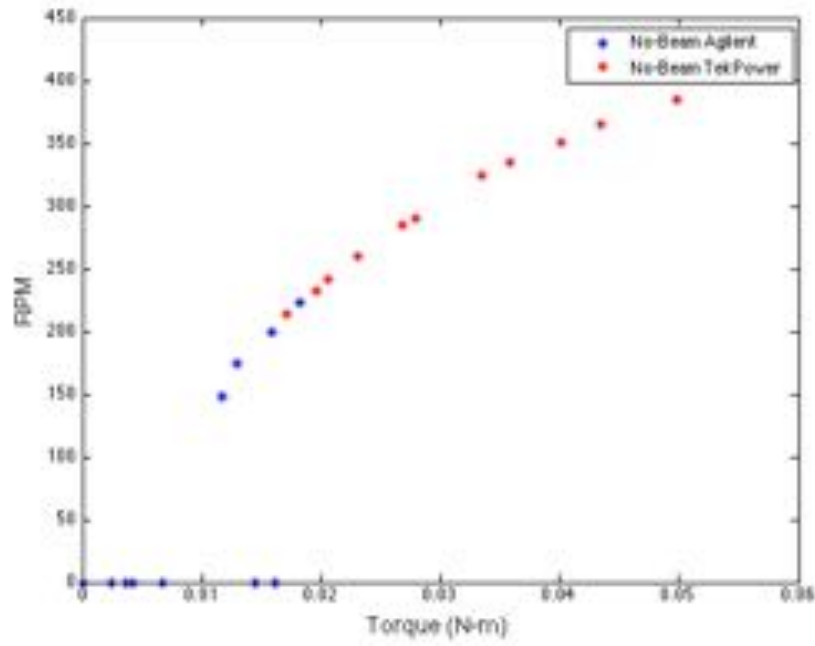


Figure 15: Motor RPM as a function of motor torque.

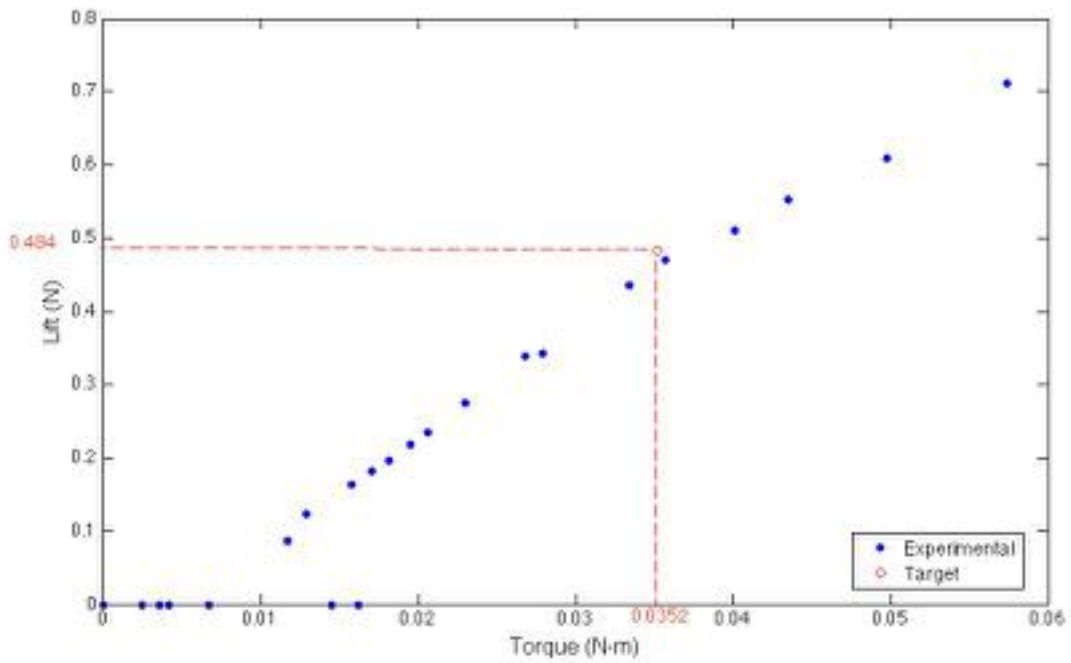


Figure 16: Lift generated as a function of input motor torque.

11 Multiple Success Points

The successes for this project are listed as follows:

1. Gained an understanding of basic helicopter aerodynamics
2. Constructed a mathematical model using MATLAB
3. Developed full-scale design
4. Applied scaling techniques using Fluid Mechanics
5. Manufactured and assembled scaled-down prototype
6. Tested prototype

To date, equations have been formulated to model a coaxial vehicle. This allows a MATLAB script to be quickly altered and output the thrust required, thrust produced, power for climb, power for hover, the Reynolds Number during hover, RPM for hover, and the required torque for climb. This allows optimization of a coaxial vehicle for the previously mentioned performance parameters. Using this script, design parameters were chosen which show that enough lift can be generated to make a rotorcraft on Mars feasible, even though the Martian atmosphere is about 1% the density of Earth's atmosphere. Figures 21 and 22 in Appendix D show the work breakdown for this project.

12 Space Grading

This project only focuses on the vertical lift aspect of the rotor mechanism; therefore, we recognize that the current prototype is not space-qualified for Mars. The following are necessary changes that need to be made before the mechanism can be fitted for a Mars rotorcraft.

- Seal rotor mechanism housing from dust particles
- Internal temperature control for motor and electronics

- Material selection
 - Strong/lightweight material for rotor blades and housing
 - Thermal insulation for electronics
 - Outgassing and depressurization
 - Vibrational Analysis
- Electrical power budget analysis
 - Battery selection
 - Radiation mitigation
- Motor selection
- Sealed thrust bearings

13 Financial Considerations

A financial breakdown can be seen below in Table 10. This breakdown is for the scaled-down prototype. The propellers themselves will be 3D printed using ABS plastic on a Dimension 3D printer and using an Objet printer. This drastically cut down on material costs and saved time. The most expensive elements of this project are the gears, bearings, and the power supply.

The cost for final design that will be operating on Mars can only be estimated at this point of the process. Since the final design will primarily be made of composites and BU's machine shop cannot handle composites, it is difficult to put a price on the manufacturing process. A preliminary breakdown of the project costs is shown in Figure 17. For such aerospace projects, the costs can typically be broken down into five categories. The two largest contributors to the mission cost are the Payload/Launch Vehicle Integration and Flight Ops/System Operations, which have to do with interfacing the payload with the launch vehicle and establishing the mission controls.¹¹

¹¹Personal correspondence with Larry Young, April 15, 2015, 12:32 PM

Table 10: Cost Summary

Part	Quantity	Vendor	Unit Cost	Shipping Cost	Total Cost
0.125" Bearing	4	Grainger	\$10.86	\$44.73	\$88.17
0.375" Bearing	1	Grainger	\$34.25	-	\$34.25
0.125" Retaining Rings	1	McMaster	\$6.30	\$11.09	\$17.39
0.375" Retaining Rings	1	McMaster	\$8.74	-	\$8.74
1" Al Rod	1	McMaster	\$38.33	-	\$38.33
Motor Coupling	1	McMaster	\$4.14	-	\$4.14
Motors	3	RobotShop	\$6.75	\$16.10	\$36.35
Gears	2	SDP-SI	\$58.79	\$16.72	\$134.30
DC Power Supply	1	Amazon	\$126.94	-	\$126.94
Total Cost					\$488.61

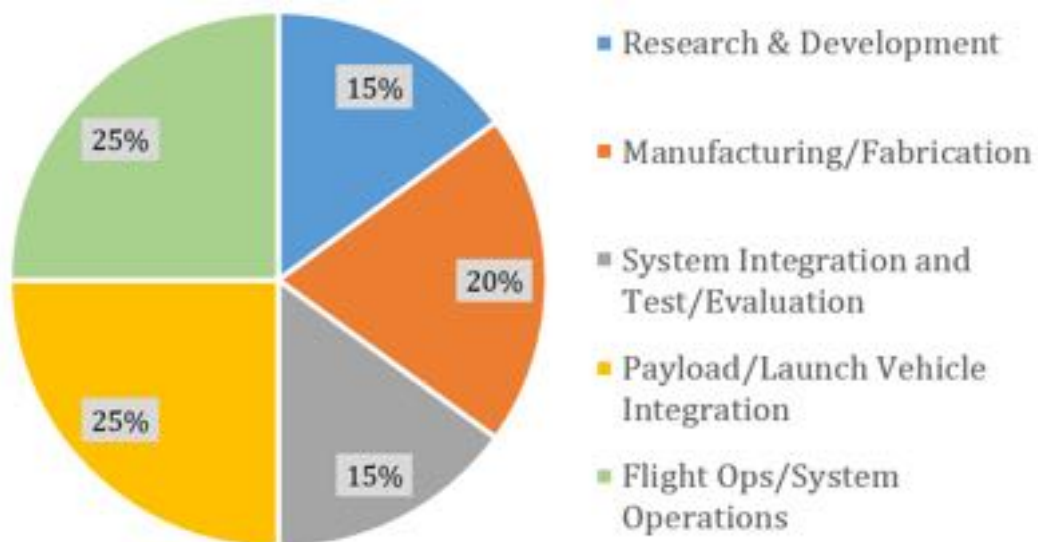


Figure 17: Breakdown of Final Mission Costs

Appendix A Calculations

This section summarizes the results of applying the theoretical methods above to the parameters defined for this project. The parameters are listed in Table 11.

Figure 18 was used to calculate the force required to climb to a height of 10 meters

Table 11: Summary of parameters used in calculations

Parameter	Value	Nomenclature
ρ (kg/m^3)	0.0155	Atmospheric Density
μ (kg/ms)	1.13E-5	Kinematic Viscosity
γ	1.3	Adiabatic Coefficient
g (m/s^2)	3.711	Gravity
R (m)	1.5	Rotor Radius
A (m^2)	7.06	Rotor Area
N	2	Number of Blades
c (m)	0.3	Chord length
M (kg)	5	Vehicle Mass
θ ($^\circ$)	30	Fixed Pitch Angle
M_{tip}	0.65	Mach Number at tip
V_{tip} (m/s)	148	Velocity at tip
Ω (rad/s)	100	Rotational Speed of Prop
a (m/s)	227	Speed of Sound
V_c	0.566	Climb Velocity

using Equation 19 where the acceleration was determined from the velocity profile in Figure 3.

$$T_{req} = M(a + g) = 20.3 \text{ Newtons} \quad (19)$$

Combining Equations 14, 15, 16, and 17 yields a thrust generated of:

$$T_{gen} = 20.8 \text{ Newtons}$$

Figure 19 (left) illustrates Equations 14, 15 and 16.

The power required for climb can be calculated using Equation 18 and Equation 20

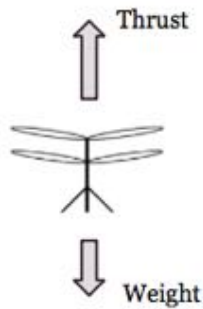


Figure 18: Free Body Diagram of the forces acting on the rover during climb.

below:

$$P_{climb} = C_p \rho A \Omega^3 R^3 = 227 \text{ Watts} \quad (20)$$

To calculate the power required for hover, recalculate C_p in Equation 18 after setting $\lambda_\infty = 0$ in Equations 14→16. This yields a power of:

$$P_{hover} = 129 \text{ Watts}$$

The RPM is calculated using:

$$RPM = \frac{60V_{tip}}{2\pi R} = 1433.6 \quad (21)$$

and the angular rotational speed, Ω is calculated as following:

$$\Omega = \frac{V_{tip}}{R} = 100.08 \text{ rad/s} \quad (22)$$

The Reynold's number varies along the propeller blade as function of the radius (Equation 23).

$$Re = \frac{\rho c \Omega r}{\mu} \quad (23)$$

Figures 19 and 20 show the Mach number and the Reynold's number as a function of the radial distance away from the center hub. The maximum Reynolds number occurs at the tip and has a value of 30,888.

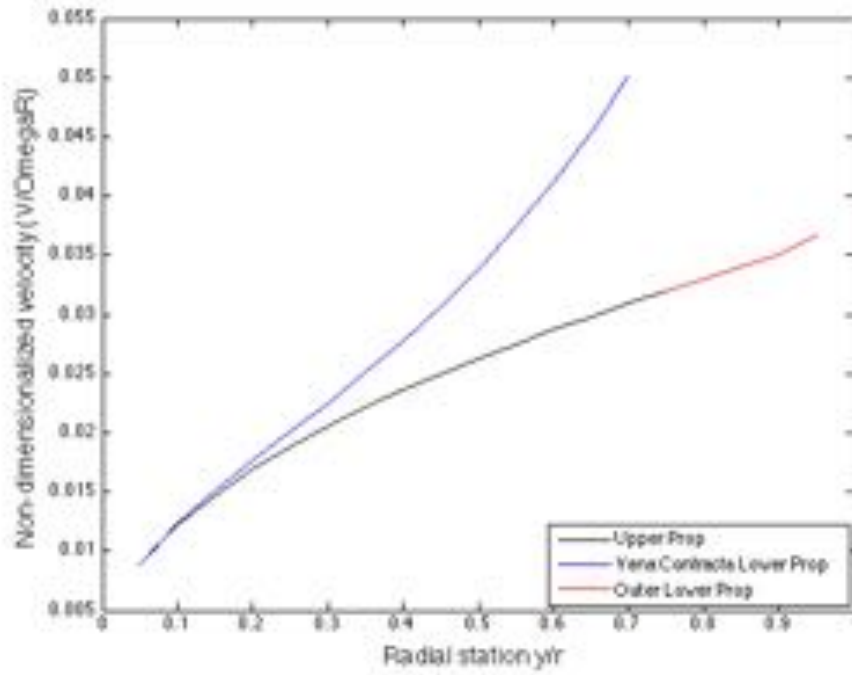


Figure 19: The induced velocity as a function of radius for the upper and lower propellers.

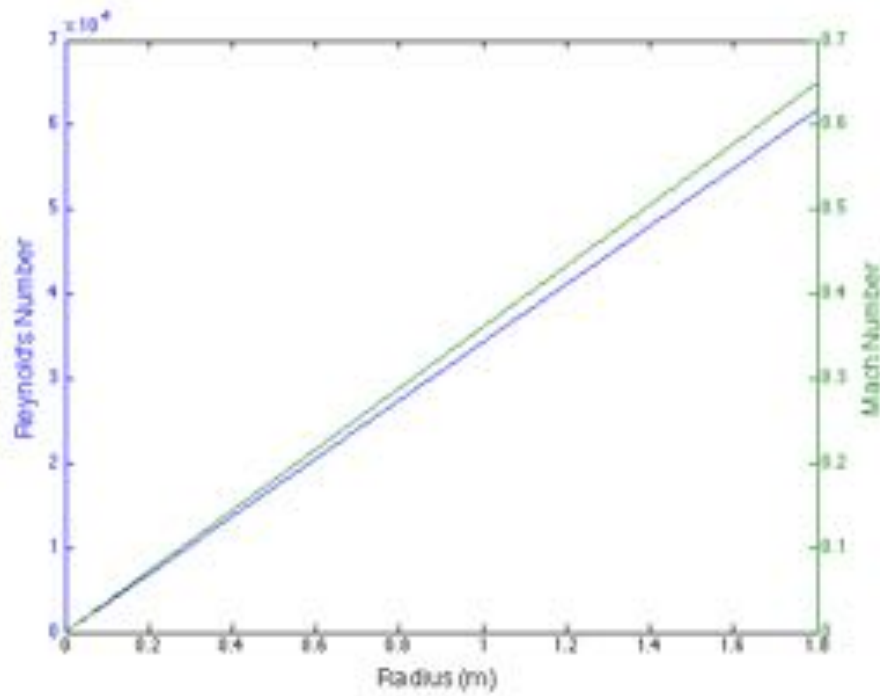


Figure 20: Reynolds Number and Mach number as a function of radius along the blade.

Appendix B Scaling

The Buckingham Pi theorem was used to scale a Mars design down to an Earth prototype. The scaling procedure focused on the torque, power, and thrust of the rotor mechanism. The final dimensions of the Earth prototype type are known (1/10 scaling factor):

$$c = 0.03m$$

$$r = 0.15m$$

First, the Reynolds number was used to scale Ω to Earth:

$$\begin{aligned} Re_{Mars} &= Re_{Earth} \\ \left(\frac{Vc}{\nu}\right)_{Mars} &= \left(\frac{Vc}{\nu}\right)_{Earth} \\ \left(\frac{\Omega Rc}{\nu}\right)_{Mars} &= \left(\frac{\Omega Rc}{\nu}\right)_{Earth} \\ \Omega_{Mars} &= \left(\frac{\Omega Rc}{\nu}\right)_{Earth} \left(\frac{\nu}{Rc}\right)_{Mars} = \frac{100.08rad/s \cdot 0.15m \cdot 0.03m}{8.316e^{-4}m^2/s} \cdot \frac{1.4604e^{-5}m^2/s}{1.5m \cdot 0.3m} \end{aligned}$$

$$\boxed{\Omega_{Earth} = 175.8rad/s}$$

The Buckingham Pi theorem was used to derive relationships that should be held constant between the two situations (Mars vs Earth). These relationships turned out to be known coefficients: C_T , C_P , and C_Q . The following calculations show the results for scaling the thrust, power and torque with the given Ω .

$$\begin{aligned} C_{T,Mars} &= C_{T,Earth} \\ \left(\frac{T}{\rho\Omega^2 R^4}\right)_{Mars} &= \left(\frac{T}{\rho\Omega^2 R^4}\right)_{Earth} \\ T_{Earth} &= \left(\frac{T}{\rho\Omega^2 R^4}\right)_{Mars} (\rho\Omega^2 R^4)_{Earth} = \frac{20.0N \cdot (1.217kg/m^3)(175.8rad/s)^2(0.15m)^4}{(0.0155kg/m^3)(100.08rad/s)^2(1.5m)^4} \end{aligned}$$

$$\boxed{T_{Earth} = 0.484N}$$

Power:

$$C_{P,Mars} = C_{P,Earth}$$

$$\left(\frac{P}{\rho\Omega^3 R^5}\right)_{Mars} = \left(\frac{P}{\rho\Omega^3 R^5}\right)_{Earth}$$

$$P_{Earth} = \left(\frac{T}{\rho\Omega^3 R^5}\right)_{Mars} (\rho\Omega^3 R^5)_{Earth} = \frac{129W \cdot (1.217kg/m^3)(175.8rad/s)^3(0.15m)^5}{(0.0155kg/m^3)(100.08rad/s)^3(1.5m)^5}.$$

$$\boxed{P_{Earth} = 0.547W}$$

Torque:

$$C_{Q,Mars} = C_{Q,Earth}$$

$$\left(\frac{Q}{\rho\Omega^2 R^5}\right)_{Mars} = \left(\frac{Q}{\rho\Omega^2 R^5}\right)_{Earth}$$

$$Q_{Earth} = \left(\frac{T}{\rho\Omega^2 R^5}\right)_{Mars} (\rho\Omega^2 R^5)_{Earth} = \frac{1.29Nm \cdot (1.217kg/m^3)(175.8rad/s)^2(0.15m)^5}{(0.0155kg/m^3)(100.08rad/s)^2(1.5m)^5}.$$

$$\boxed{Q_{Earth} = 0.031Nm}$$

Appendix C Testing Calculations

The angular velocity on Earth was used to find the required motor torque for the scaled prototype. The angular velocity is constant at the top of the velocity profile curve in Figure 3. The time it takes to reach that constant velocity is 1.6 seconds. The angular acceleration can then be found by using the relation:

$$\alpha = \frac{\Omega_{Earth}}{1.6sec} = 109.8 \text{ rad/s}^2$$

The torque can be found by:

$$\tau = J \cdot \alpha$$

where J is the rotary moment of inertia. This can be found by analyzing each part of the system determine how its mass and radius will contribute to the overall inertia. The following parts contribute to the inertia:

1. Blades
2. Inner Shaft
3. Outer Shaft
4. Drive Shaft
5. Coupling
6. Gears
7. Top Hub
8. Screws

The total rotary moment of inertia is $J = 3.209 \cdot 10^{-4} kg \cdot m^2$. Therefore, the required torque is:

$$\tau = 109.8 \text{ rad/s}^2 \cdot 3.209 \cdot 10^{-4} \text{ kgm}^2 = 0.03524 \text{ N-m} = 4.99 \text{ oz-in}$$

A motor with a torque of at least 4.99 oz-in was selected for the prototype. To determine the current that must be applied to achieve the required torque. The torque constant for this motor (from the spec sheet) is 0.83 oz-in/A. Therefore, the required current is:

$$I = \frac{4.99\text{oz-in}}{0.83\text{oz-in/A}} = 6.01A$$

Appendix D Gantt Charts

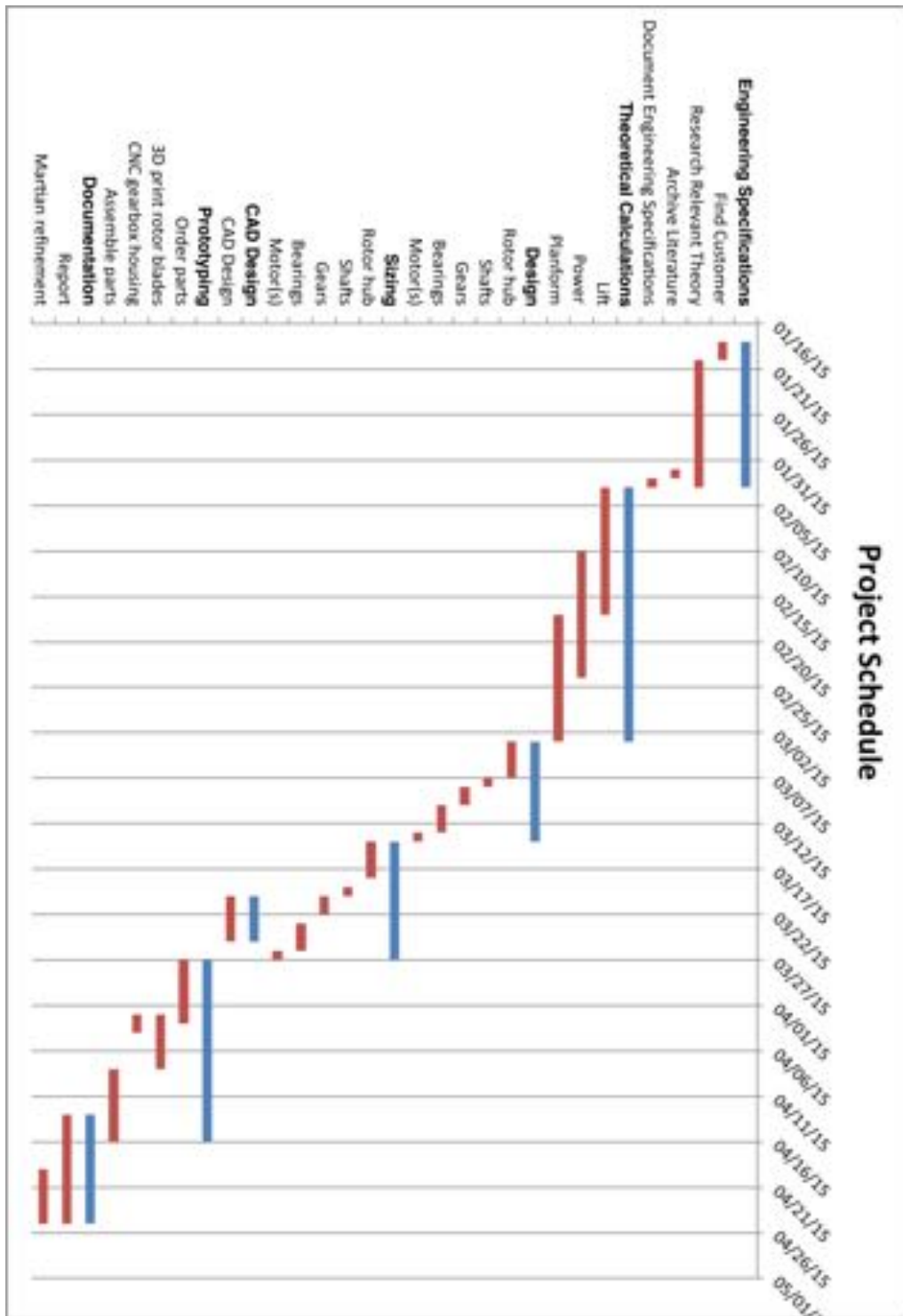


Figure 21: Detailed Gantt chart of project.

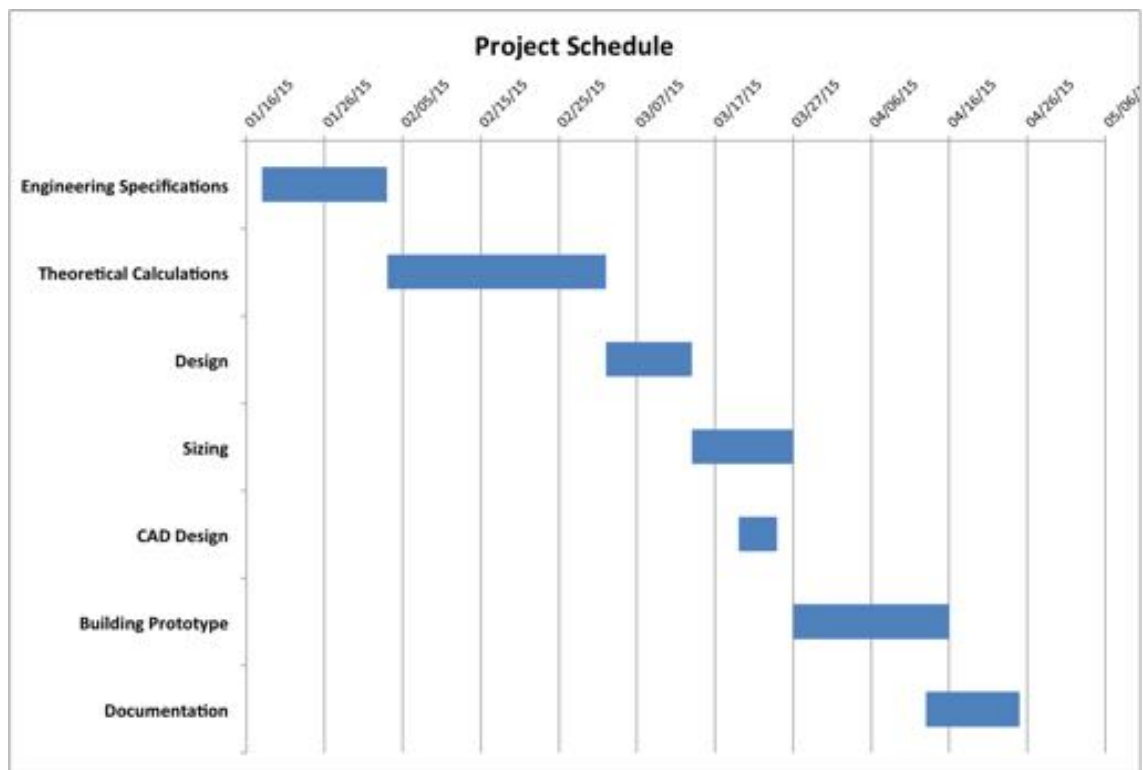


Figure 22: Abbreviated Gantt chart of project.

Appendix E Space Grading

Figure 23 shows a comparison of the radiation experience on Earth compared to Mars¹².

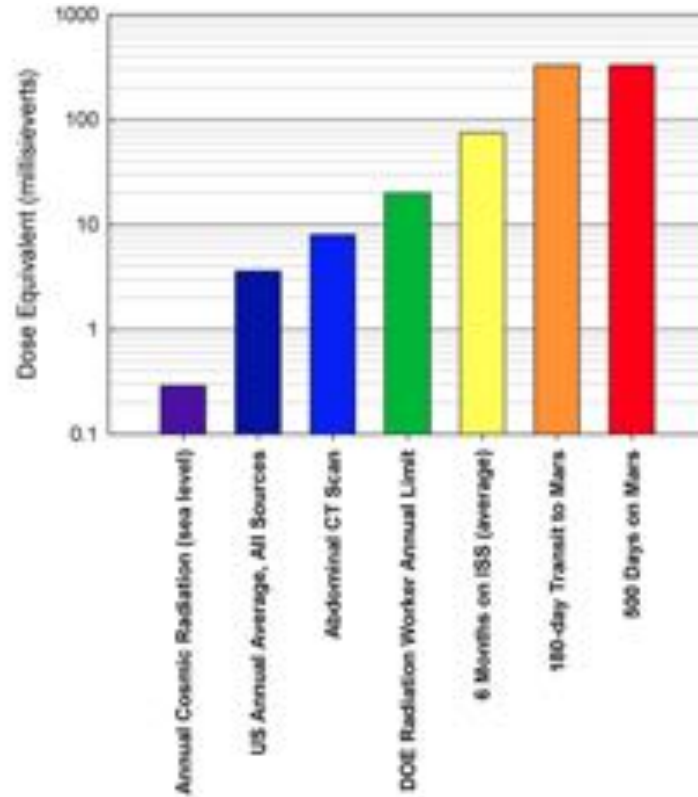


Figure 23: Radiation comparison between Earth and Mars.

¹²<http://www.space.com/24731-mars-radiation-curiosity-rover.html>

Appendix F Scaled Design Drawings

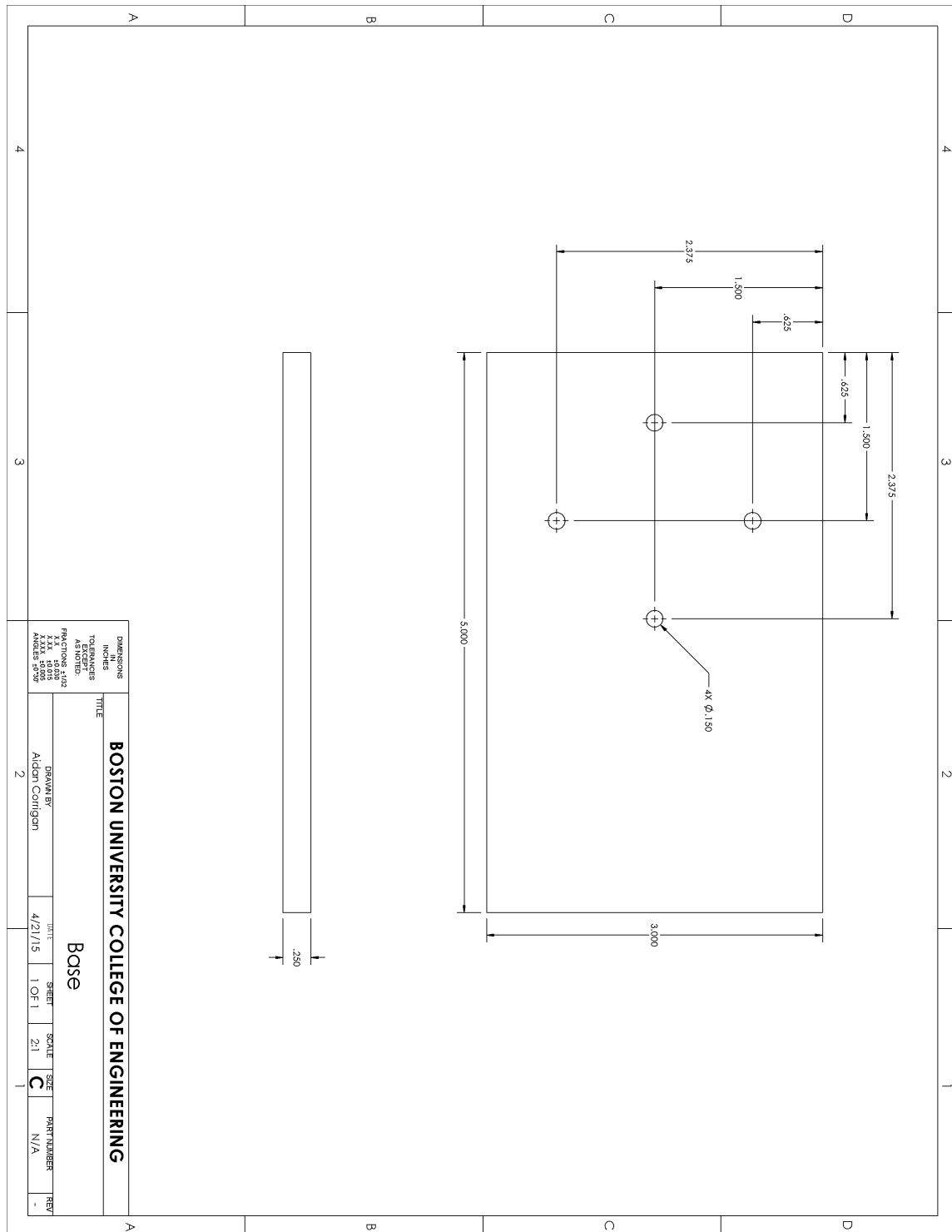


Figure 24: Schematic Drawing of the Base Plate.

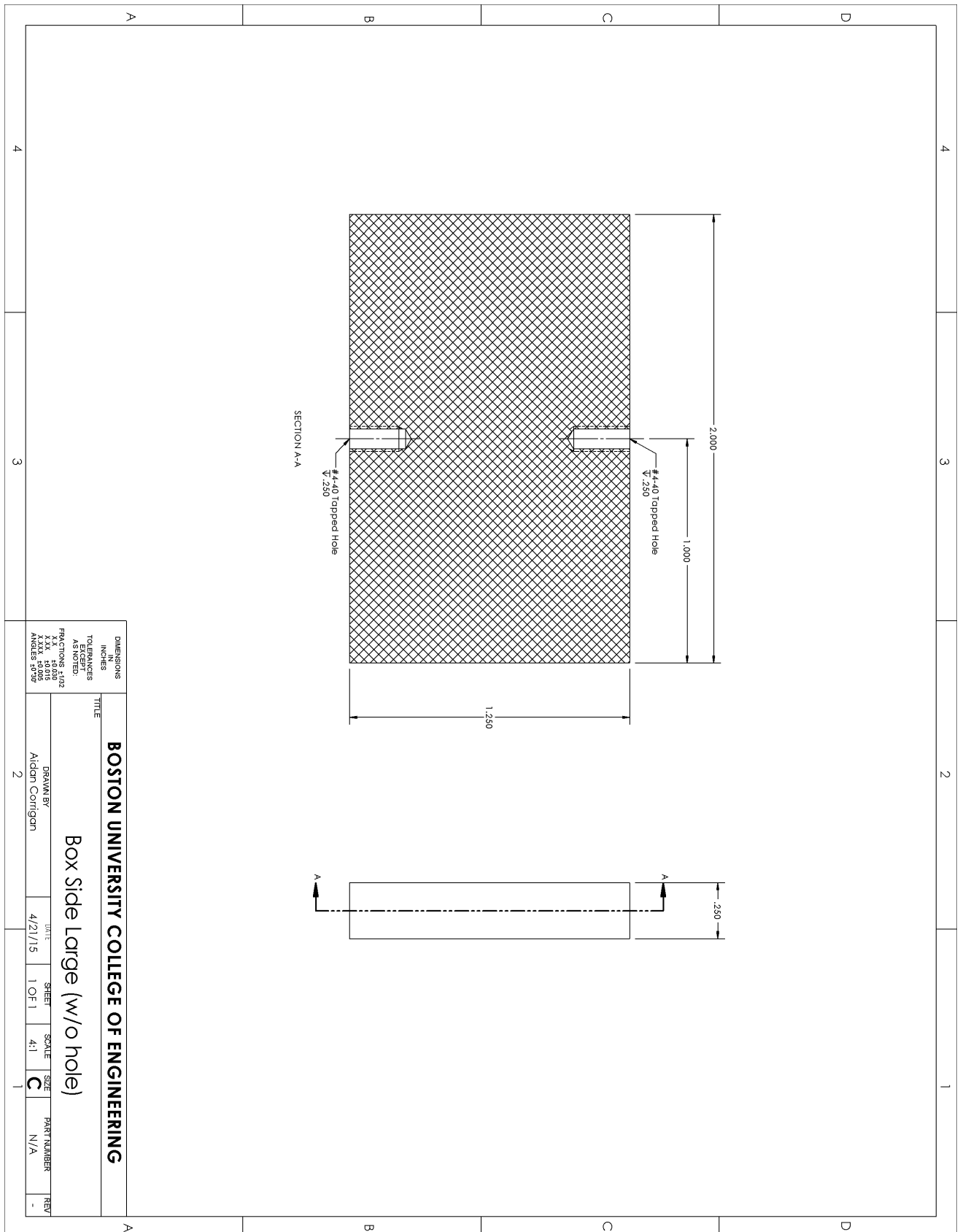


Figure 26: Schematic Drawing of a Side of the Gear Box.

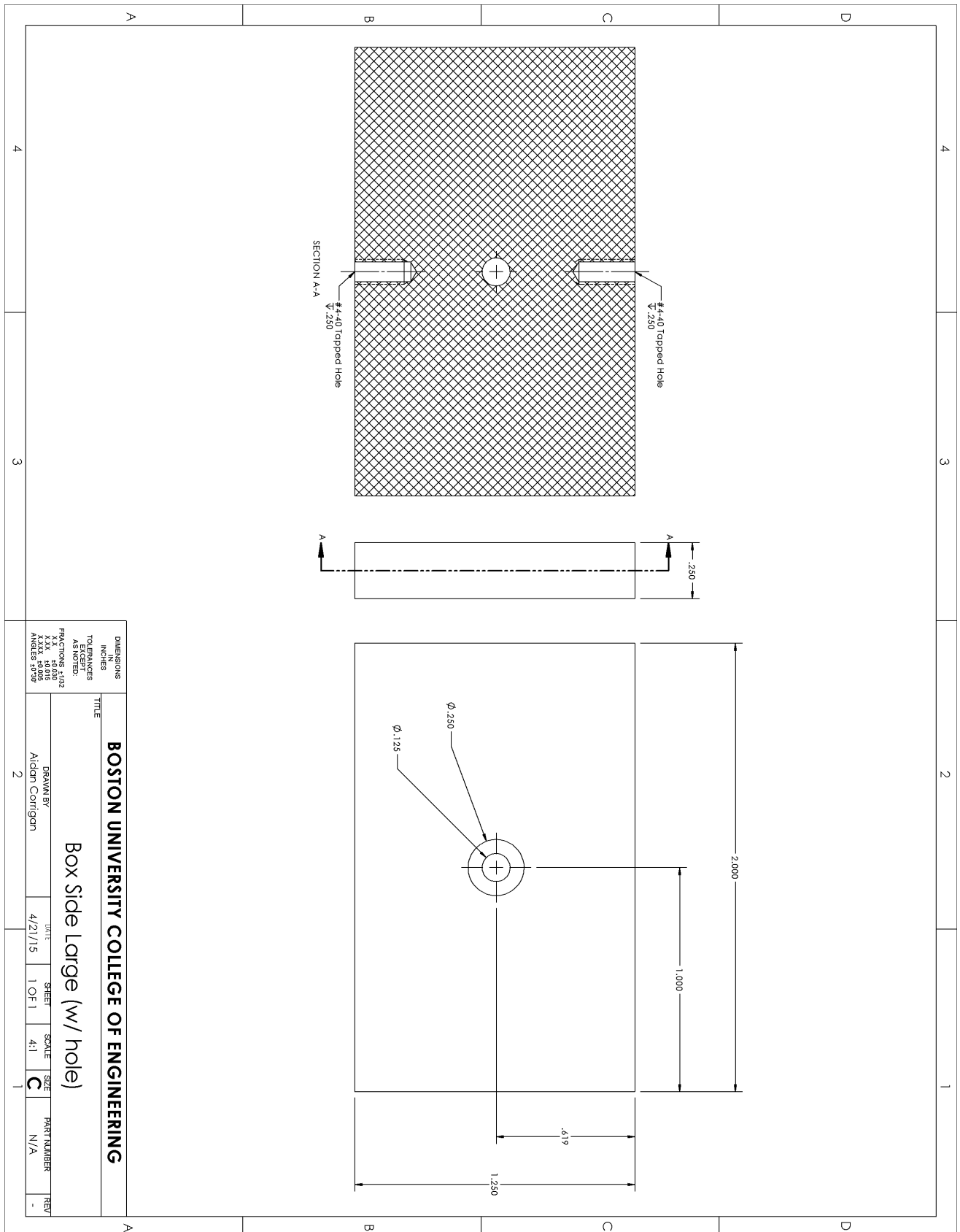


Figure 27: Schematic Drawing of a Side of the Gear Box.

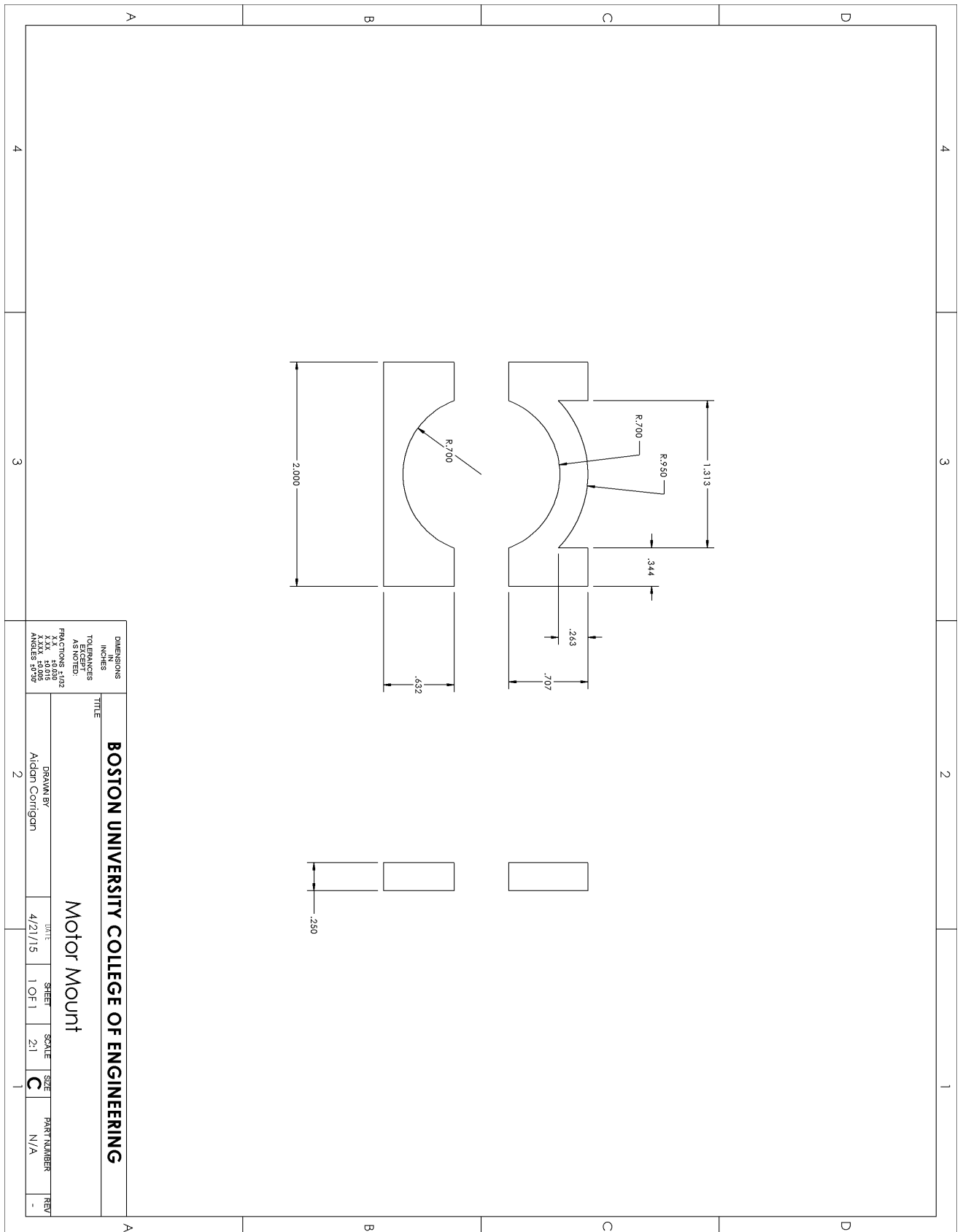


Figure 30: Schematic Drawing of the Motor Mount.

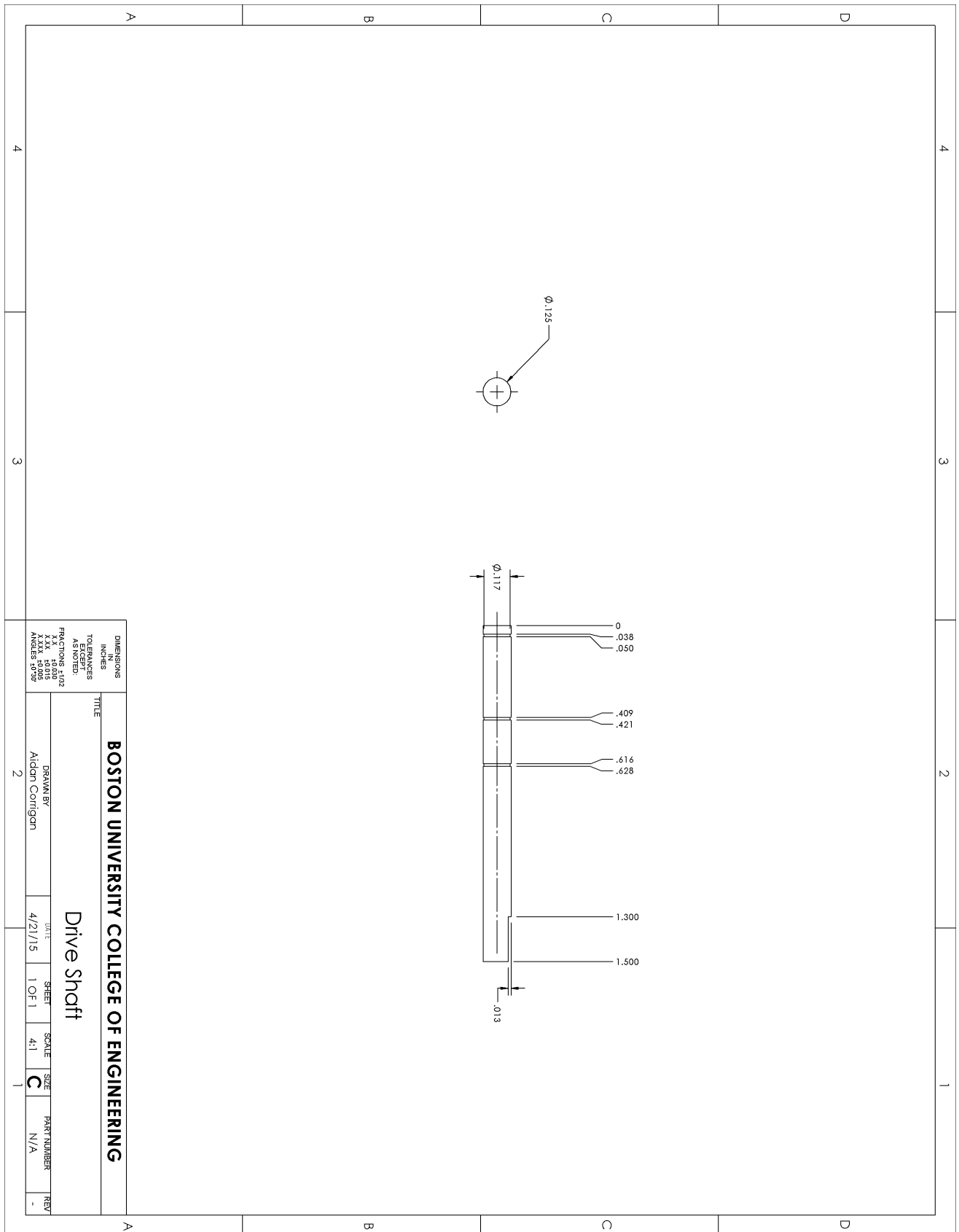


Figure 31: Schematic Drawing of the Drive Shaft.

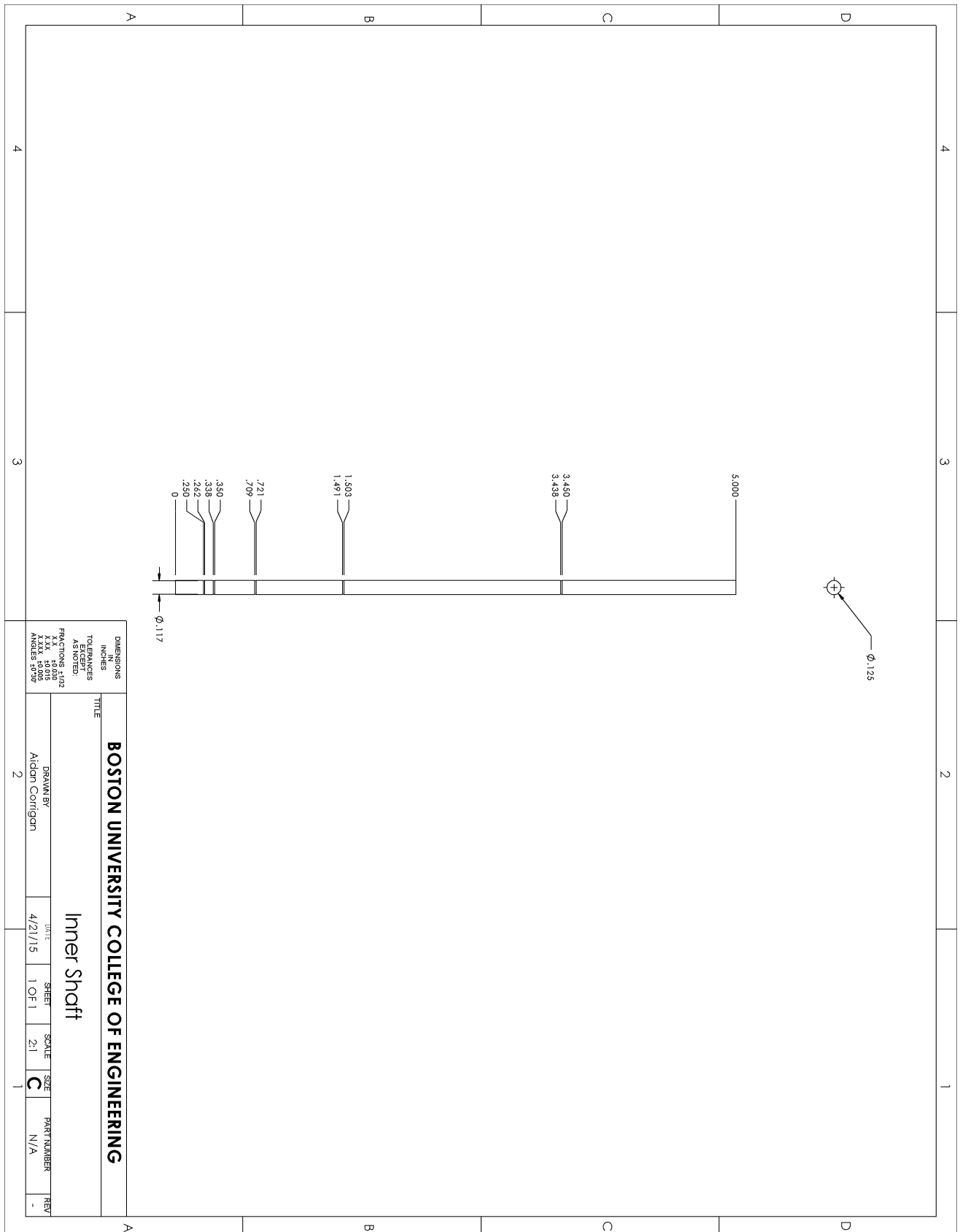


Figure 32: Schematic Drawing of the Inner Shaft.

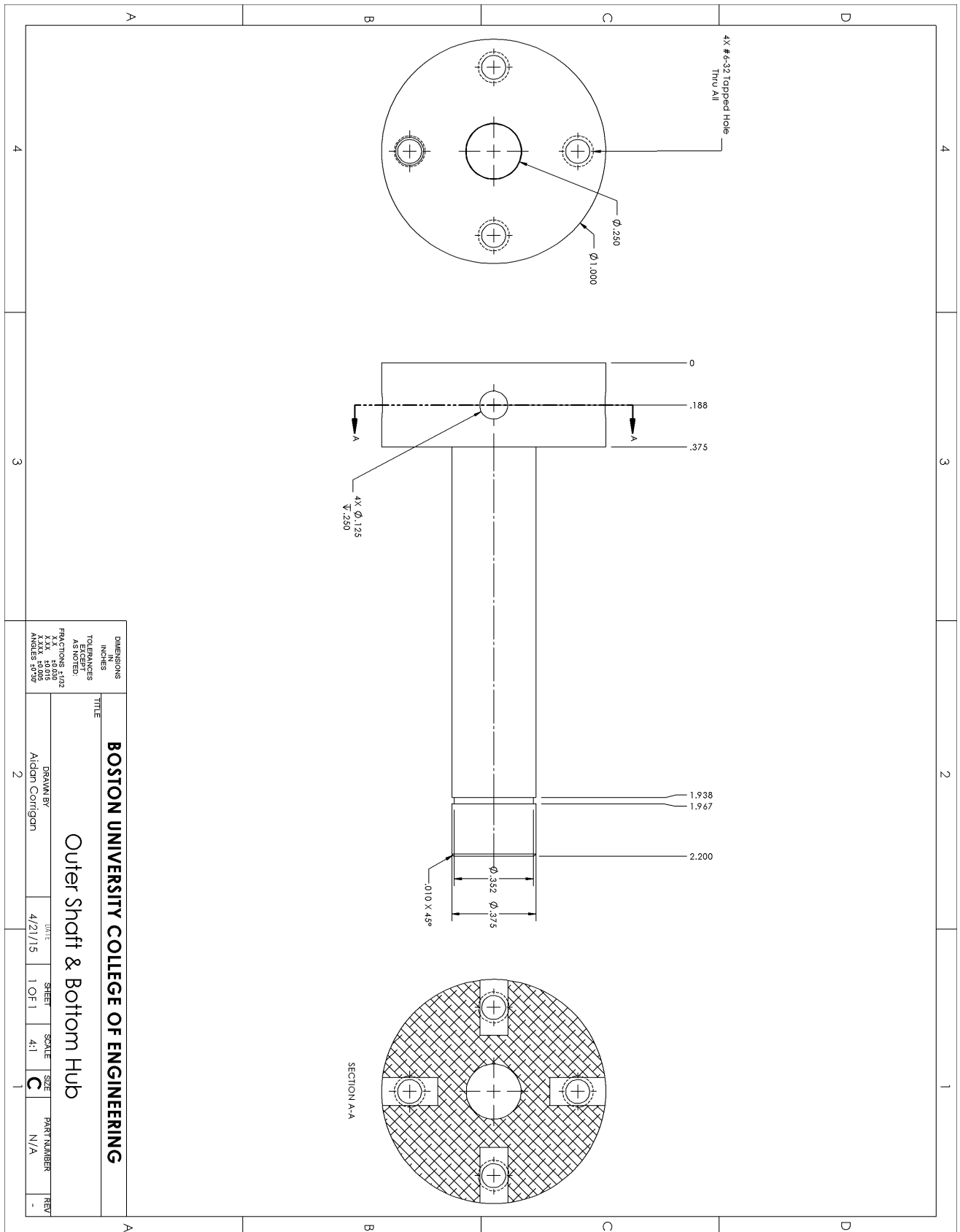


Figure 33: Schematic Drawing of the Outer Shaft.

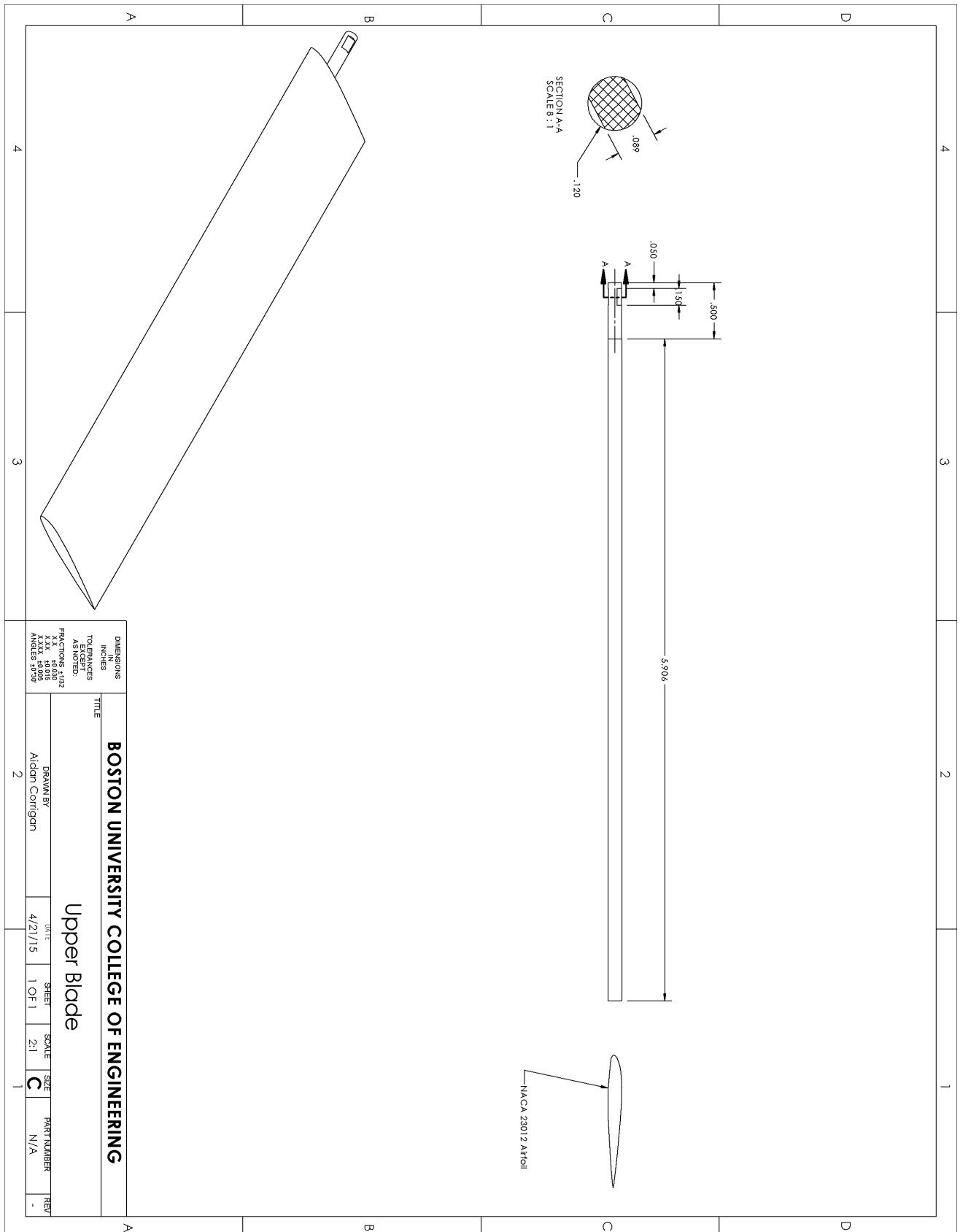


Figure 34: Schematic Drawing of an Airfoil.

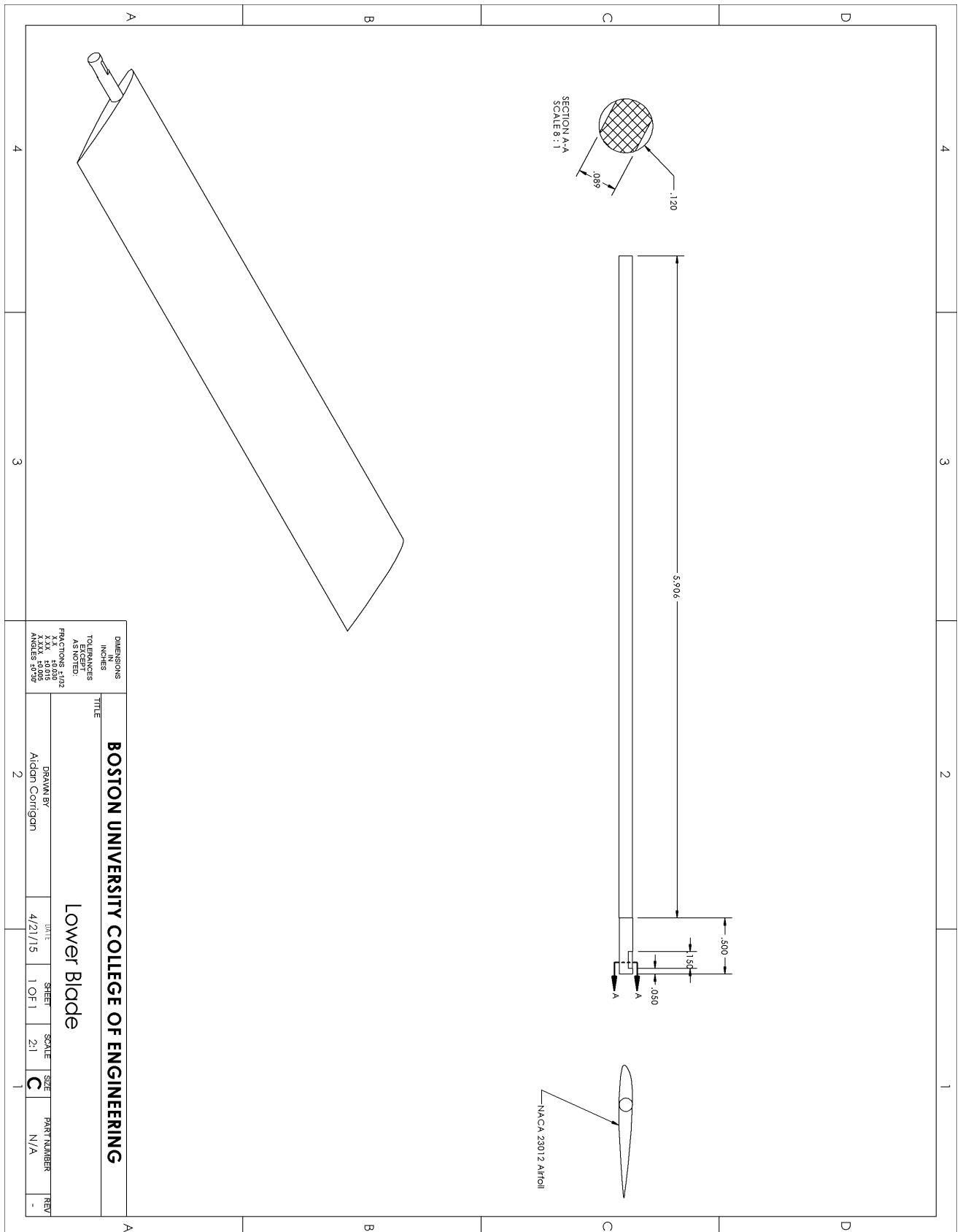


Figure 35: Schematic Drawing of an Airfoil.

Appendix G Ordered Part Specifications

High-Strength 2024 Aluminum
1" Diameter



Length, ft. 2 Each

In stock
 \$38.33 Each
 86885K58

Alloy	2024
Shape	Rod
Finish	Unpolished
Diameter	1"
Diameter Tolerance	±0.012"
Yield Strength	45,000 psi
Hardness	Soft (120 Brinell)
Material Condition	Heat Treated
Temper	T351
Specifications Met	AMS 4120, AMS QQ-A-225/6, ASTM B211
Material Composition	
Silicon	0-0.5%
Iron	0-0.5%
Copper	3.8-4.9%
Manganese	0.3-0.9%
Magnesium	1.2-1.8%
Chromium	0-0.1%
Zinc	0-0.25%
Titanium	0-0.15%
Other	0-0.15%
Aluminum	90.75-94.7%
Nominal Density	0.101 lbs./cu. in.
Modulus of Elasticity	10.6 ksi = 10 ³
Elongation	10-20%
Melting Range	935° to 1,160° F
Thermal Conductivity	840 Btu/ft. · in./sq ft. @ 75° to 77° F
Electrical Resistivity	30-35 Ohm-Cir. Mil/ft.
Length Tolerance	±1"
Length	2 ft.
Length	2 ft.

Figure 36: Aluminum Rod Specifications.

1 INCH
50DP

MITER GEARS • 72 PITCH
AGMA 101 | 1/8 BORE | PRECISION MATCHED SETS | 20° PRESSURE ANGLE | RATIO 1:1

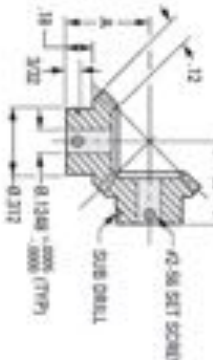


MATERIAL:
202 Stainless Steel
2024-T4 or -T351 Aluminum Alloy
anodized before cutting.

Available on special order:
Different bore size and/or material, precision by
Standard Steel.

Sold as Set

Catalog Number	No. of Teeth	P.O.	A	Material
Pin Type				
ST1802-TREKMAN04	24	303	437	Stainless Steel / Aluminum
ST1802-TREKMAN04	36	303	437	Stainless Steel
ST1802-TREKMAN04	36	303	437	Aluminum
ST1802-TREKMAN06	36	508	521	Stainless Steel / Aluminum
ST1802-TREKMAN06	36	508	521	Stainless Steel
ST1802-TREKMAN08	36	508	521	Aluminum
Clamp Type				
ST1802-TREKMAN04	24	303	489	Stainless Steel / Aluminum
ST1802-TREKMAN04	36	303	489	Stainless Steel
ST1802-TREKMAN04	36	303	490	Aluminum
ST1802-TREKMAN06	36	508	500	Stainless Steel / Aluminum
ST1802-TREKMAN06	36	508	500	Stainless Steel
ST1802-TREKMAN08	36	508	500	Aluminum



Pin Type



Clamp Type

TEL: PHONE: 518.208.1300 • FAX: 518.208.8027 • WWW.SSP-SC.COM

Figure 37: Bevel Gear Specifications.



How can we improve our Product Images?

[Compare](#)

Mini Ball Bearing, Shielded, Bore 0.3750in

DYNAROLL

Price ⓘ
\$34.25 / each

Deliver one time only
 Auto-Reorder Every ⓘ

[Add to Cart](#)
[+ Add to List](#)

Confirm ZIP Code to determine availability.
 ZIP Code [Save](#)

☆☆☆☆☆ [Be the first to write a review](#) | [Ask & Answer](#)

Item # **1ZQA1** Mfr. Model # **SR620ZZ A5** UNSPSC # **31171504**

Catalog Page # **203** Shipping Weight **0.001 lbs.**

Country of Origin **Japan** | Country of Origin is subject to change
Note: Product availability is real-time updated and adjusted continuously. The product will be reserved for you when you complete your order. [More](#)

Static Load Capacity (Lb.)	50
Max. RPM	30,000
Temp. Range (F)	-65 - 250
Cage Material	Stainless Steel
Material	Stainless Steel
Shield Material	Stainless Steel
Lubrication	Oil

Technical Specs

Item	Miniature Ball Bearing
Type	Shielded, Unflanged
Bore Dia.	0.3750 in.
Outside Dia.	0.6250 in.
Width	0.1562 in.
ABEC Tolerance	5
Dynamic Load Capacity (Lb.)	93

Figure 38: Large Ball Bearing Specifications.



Mini Ball Bearing, Shielded, Bore 0.1250in

DYNAROLL

Price ①
\$10.86 / each

Deliver one time only
 Auto-Reorder Every 1 Month ⓘ

Add to Cart + Add to List

Confirm ZIP Code to determine availability.
 ZIP Code Save

★ ★ ★ ★ ★ Be the first to write a review | Ask & Answer

Item # **1ZER8** Mfr. Model # **SR144ZZ AS** UNSPSC # **31171504**
 Catalog Page # **202** Shipping Weight **0.01 lbs.**

Country of Origin **Japan** | Country of Origin is subject to change
 Note: Product availability is real-time updated and adjusted continuously. The product will be reserved for you when you complete your order. [More](#)

Technical Specs

Item	Miniature Ball Bearing	Max. Load Axial (Lb.)	21
Type	Shielded, Unflanged	Max. RPM	80,000
Bore Dia.	0.1250 in.	Temp. Range (°F)	-65 - 250
Outside Dia.	0.2500 in.	Cage Material	Stainless Steel
Width	0.1094 in.	Material	Stainless Steel
AFFC Tolerance	5	Shield Material	Stainless Steel
Dynamic Load Capacity (Lb.)	64	Lubrication	Oil
Static Load Capacity (Lb.)	20		

Figure 39: Small Ball Bearing Specifications.

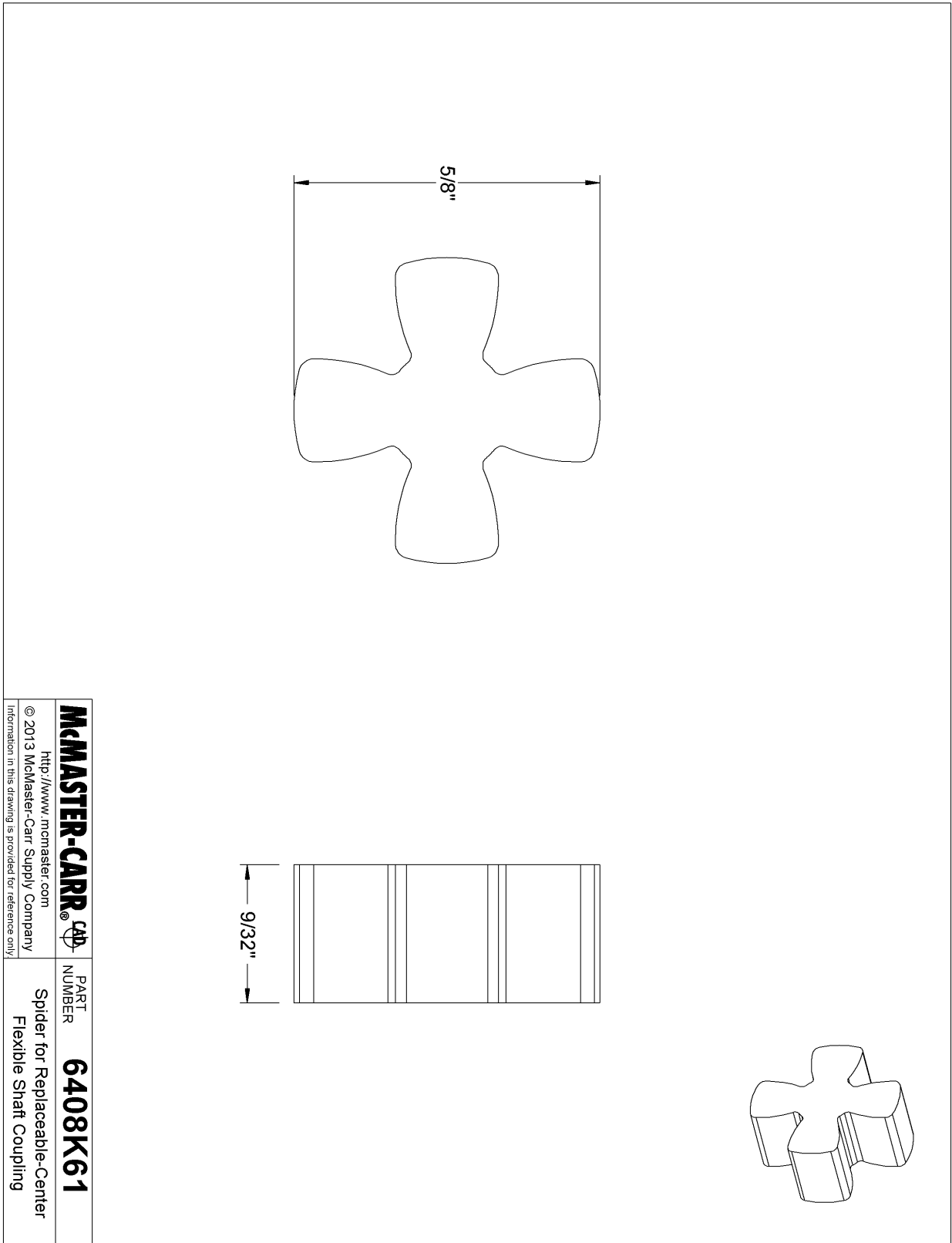


Figure 40: Coupling Spider Specifications.

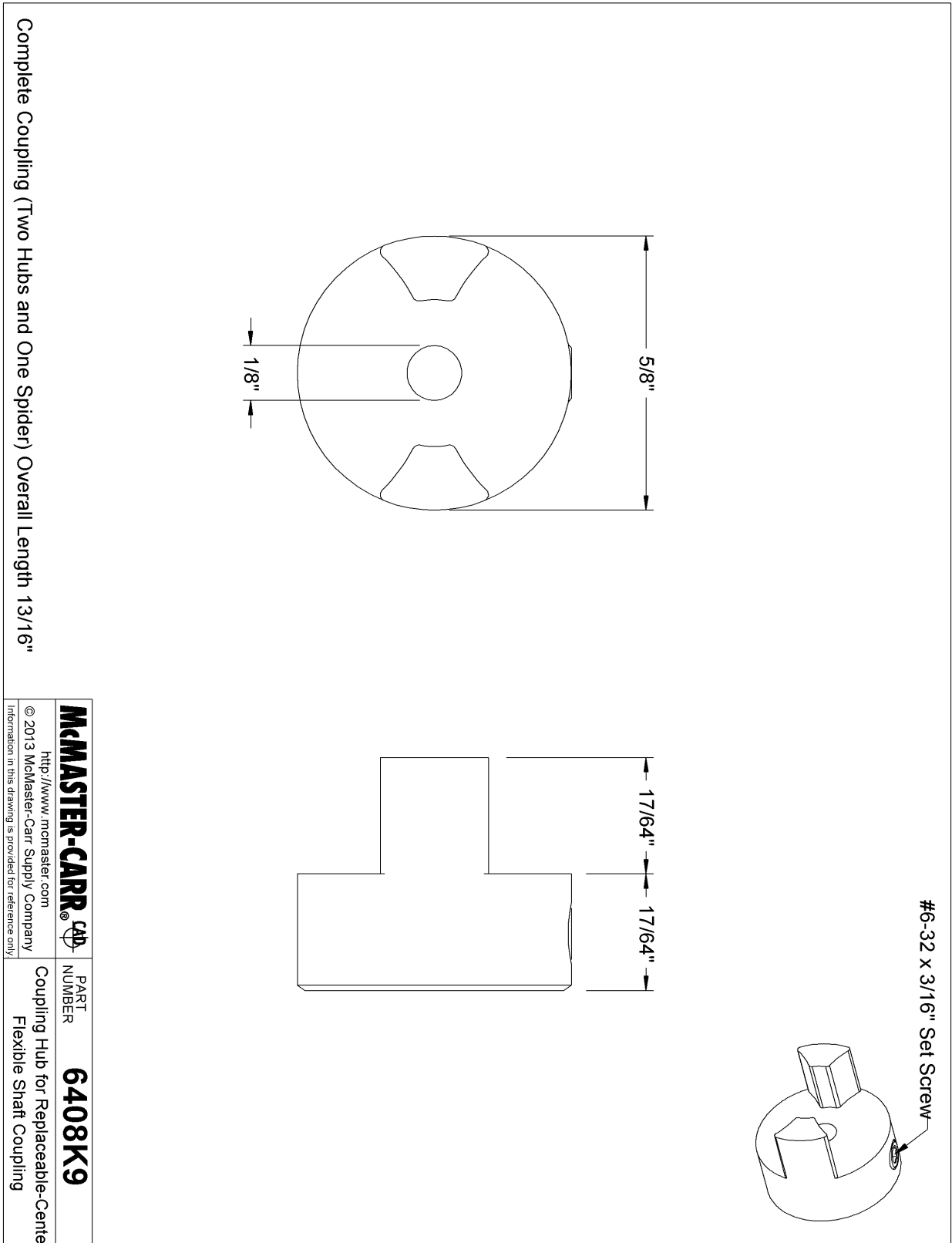


Figure 41: Coupling Hub Specifications.

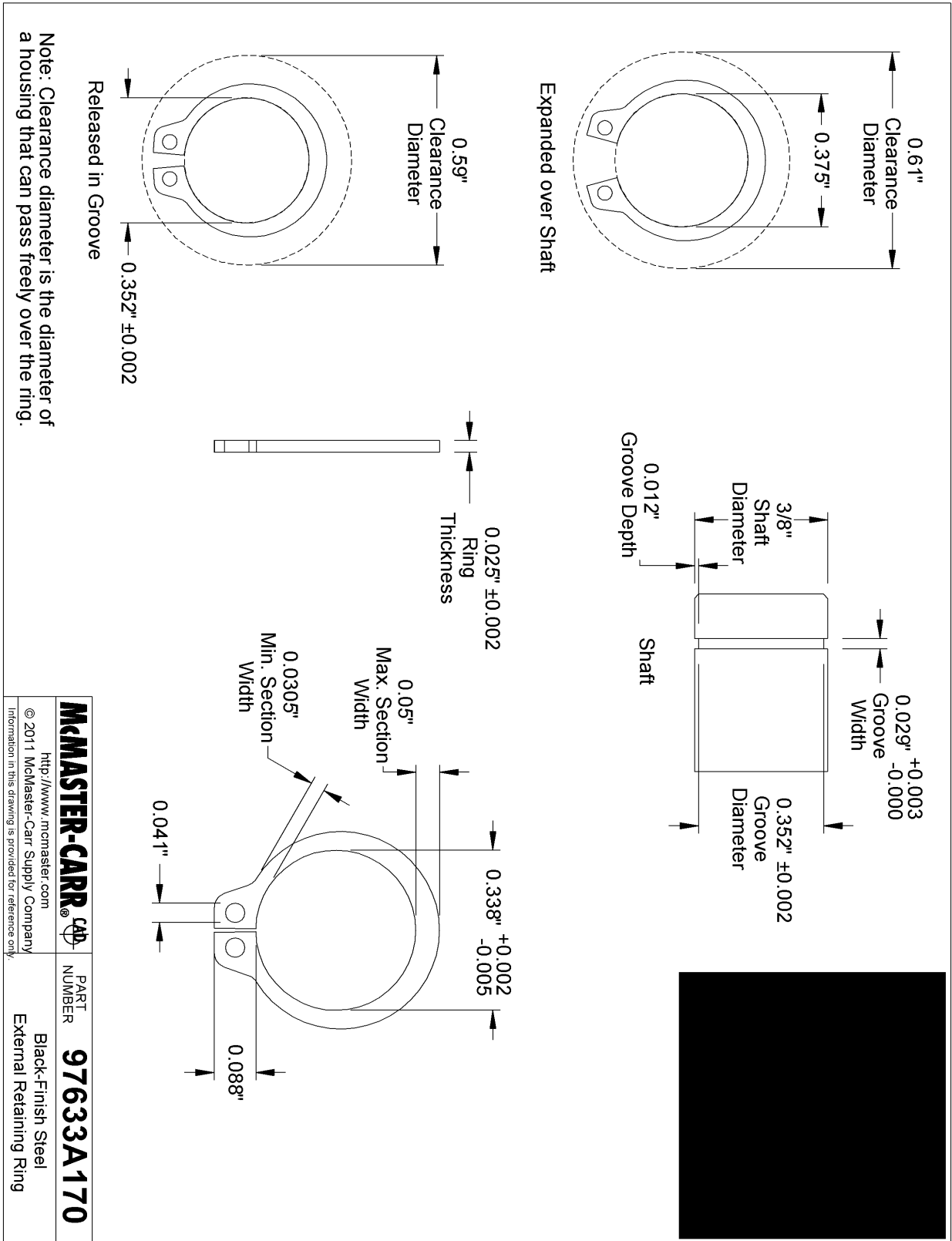


Figure 42: Large Retaining Ring Specifications.

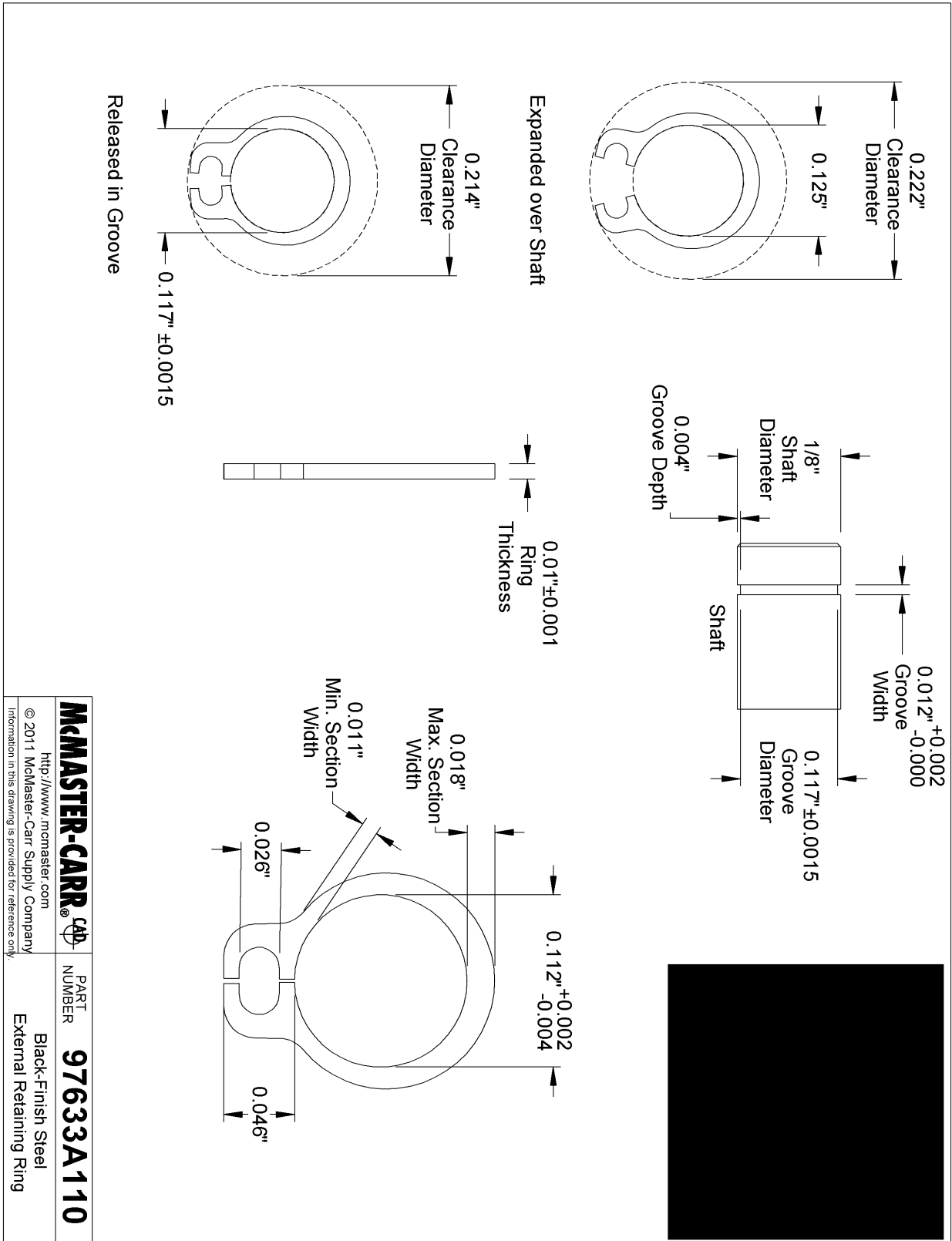


Figure 43: Small Retaining Ring Specifications.

Description

- Powerful Mabuchi RS-550 DC Motor
- 85A stall current
- 6 to 14.4V input range (12V nominal)

This is the powerful **Banebots RS-550 DC Motor** with a 3-pole balanced armature. This motor can also be purchased with a choice of planetary gearheads which reduces the speed and increases torque. If you are using this motor with a microcontroller, you will need a powerful motor controller.

Specifications

- Operating Voltage: 6 - 14.4V (12V Nominal)
- No Load RPM: 19300
- No Load Current: 1.2A
- Stall Torque: 70.55oz-in (498.2mN-m)
- Stall Current: 85A
- Kv: 0.83oz-in/A (0.9mN-m/A)
- Kv: 1628 rpm/V
- Efficiency: 70%
- RPM Peak Efficiency: 17250
- Current Peak Efficiency: 10A

[Back to top](#)



Specifications

- Powerful Mabuchi RS-550 DC Motor
- 85A stall current
- 6 to 14.4V input range (12V nominal)

Product Code : RB-Ban-80 by [Banebots](#)

★★★★★ (2)

Banebots RS-550 Motor 19300rpm 12V 70.55oz-in

Product Code : RB-Ban-80 by [Banebots](#)

★★★★★ (2)

- Powerful Mabuchi RS-550 DC Motor
- 85A stall current
- 6 to 14.4V input range (12V nominal)

Dimensions

- Weight: 7.7oz (218g)
- L: 2.24in (57mm) D: 1.52in (38.5mm)
- Shaft Diameter: 0.12in (3.2mm)
- Shaft Length: 0.2in (7.6mm)
- Mounting holes (2): M3

Supplier Product Code

MS-RS550-12

[Back to top](#)

Supplier Product Code

MS-RS550-12

[Back to top](#)

Figure 44: Motor Specifications.

Appendix H Manufacturing Procedure

Parts List:

- DC Brushed Motor
- 0.125" Retaining Rings
- 0.375" Retaining Rings
- 2', 1" Al 2024 Rod
- 0.125" Al 2024 Rod
- 2 sets of Bevel Gears
- 0.125" Bearing
- 0.375" Bearing
- 3D Printed Propeller Blades
- 4-40 Screws

Procedure:

1. Machine retaining rings grooves and slots on 0.125" Al shaft (per drawing)
2. Place right retaining ring on 0.125" shaft
3. Press fit 0.125" bearing onto 0.125" shaft from the left up until the retaining ring from Step 2
4. Machine outer 1" Al shaft to drawing specs
5. Press fit outer shaft to bearing on inner shaft (from Step 3).
6. Press fit 0.125" bearing between inner and outer shafts such that the top of the bearing is flush with the shoulder in the outer shaft
7. Place the 0.125" retaining ring on inner shaft flush with the bearing from Step 6

8. Slide top gearbox housing onto outer shaft
9. Press fit 0.375" bearing onto outer shaft
10. Place 0.375" retaining ring onto outer shaft
11. Slide bored out bevel gear into place between inner and outer shaft
12. Screw onto outer shaft
13. Place 0.125" retaining ring in the middle groove on 0.125" shaft
14. Slide bevel gear flush with retaining ring from previous step and screw into place
15. Place retaining ring on other side of bevel gear
16. Press fit 0.125" bearing into bottom gearbox housing
17. Place 0.125" retaining ring on leftmost side of 0.125" shaft
18. Press fit 0.125" shaft into 0.125" bearing in lower box housing
19. Machine grooves and slots into 0.125" drive shaft
20. Press fit 0.125" bearing into side gearbox housing
21. Place retaining ring on the drive shaft next to bearing from previous step
22. Place 0.125" retaining ring on the middle groove of the drive shaft
23. Slide drive bevel gear onto drive shaft and screw into place
24. Place 0.125" retaining ring on the other side of the drive bevel gear
25. Screw together gearbox housing using 4-40 screws (0.75" long)
26. Attach flexible coupling to the drive shaft from the gearbox housing and the motor output shaft

Appendix I MATLAB Code

```

clear
clc
close all
%% Input Parameters
% Atmospheric Properties
rho = 0.0155; %Density (kg/m^3)
mu = 1.13e-5; %kinematic viscosity kg/m s
gamma = 1.3; %Gamma for CO2
pressure = 636; %Pressure in Pa
g = 3.711; %Martian gravity (m/s^2)

% Physical Parameters
R = 1.8 ; %Radius (m)
A = pi*R^2; %Rotor area (m2)
N = 4 ; %Total Number of blades
c = .3; %Chord length (m)
sigma = (N*c)/(pi*R); %Rotor solidity (dimensionless)
M = 5; %Mass of UAV in kg
%theta = (70:-1.5:40)*(pi/180); %Variable Pitch (radians)
ftheta = 35*(pi/180); %Fixed Pitch (radians)

% Speeds
Mtip = .65; %Mach number at tip
a = sqrt((gamma*pressure)/(rho)); %Speed of sound (m/s)
Vtip = Mtip*a; %Tip speed of rotor (m/s)
Omega = Vtip/R; %Rotational Speed of Rotor (rad/s)
tup = 20; %Time to raise to max height
Vc = .556; %Inflow velocity (m/s) / Vclimb

```

```

lambdainf = Vc/(Omega*R);           %Non dimensional velocity
r = 0:.05:1;                        %Radius vector, non
    dimensionalized

%Airfoil
cdo = 0.021;                         %Zero lift drag coefficient (based
    on airfoil)
Cla = 0.10769;                       % Clalpha
k = 1.1;                             %induced power factor
kint = 1.219;                       %induced power interference factor
Cla = 0.08;                          %Lift Curve Slope (NACA 23012)
alpha = .8;                          %Angle of attack degrees

%% Thrust
%Required Thrust
%Use FBD to find thrust required to lift to 10 m in 4s
aup = Vc/2; %m/s^2 for 2 seconds. see velocity profile
T = M*aup+M*g;
fprintf('The Thrust required for hover is %.01f N \n',T)
% Upper Rotor Calculations
F = 1;
for j = 1:5
lambdau = sqrt(((sigma*Cla)./(16*F)-lambdainf/2).^2+((sigma*Cla*
    ftheta.*r)./(8*F)))-((sigma*Cla)./(16*F)-lambdainf/2);
phi = lambdau./r; %Induced flow angle
f = (N/2)*((1-r)./(r.*phi));
F = (2/pi)*acos(exp(-f));

end
% Lower Rotor

```

```

Ac = pi*.707^2;
% r 1 - 15
Acen = pi*r(1:15).^2;
Fcen = F(1:15);
rcen = r(1:15);
lcenu = lambdau(1:15);
%thetacen = theta(1:15);
lambdalc = sqrt(((sigma*Cla)./(16*Fcen)-(lambdainf+(Acen/Ac).*
    lcenu)/(2)).^2+(sigma*Cla.*ftheta.*rcen)./(8*Fcen))-((sigma*Cla
    )./(16*Fcen)-(lambdainf+(Acen/Ac).*lcenu)/(2)));
phicen = lambdalc./rcen;
fcen = (N/2)*((1-rcen)./(rcen.*phicen));
Fcen = (2/pi)*acos(exp(-fcen));
% r = 16 - 20;
Aout = pi*r(16:end).^2;
Fout = F(16:end);
rout = r(16:end);
loutu = lambdau(16:end);
%thetaout = theta(16:end);
lambdalo = sqrt(((sigma*Cla)./(16*Fout)-lambdainf/2).^2+((sigma*
    Cla*ftheta.*rout)./(8*Fout)))-((sigma*Cla)./(16*Fout)-lambdainf
    /2));
% Finding Ct
intup = lambdau.^2.*r;
Ctup = sum(intup(intup>0)*.05);
intlowcen = lambdalc.^2.*rcen;
Ctlowcen = sum(intlowcen(intlowcen>0)*.05);
intlowout = lambdalo.^2.*rout;
Ctlowout = sum(intlowout(intlowout>0)*.05);
Ct = 4*(Ctup+Ctlowcen+Ctlowout);

```

```

%finding Cp
inpup = intup.*lambdau;
Cpup = sum(inpup(inpup>0*.05));
inplowcen = intlowcen.*lambdalc;
Cplowcen = sum(inplowcen(inplowcen>0)*.05);
inplowout = intlowout.*lambdalo;
Cplowout = sum(inplowout(inplowout>0)*.05);
Cp = 4*(Cpup+Cplowcen+Cplowout);
Thrust = Ct*rho*A*Omega^2*R^2;
Power = Cp*rho*A*Omega^3*R^3;

%Finding lambda for hover. lambda_inf=0
% Upper Rotor Calculations
F_h = 1;
for j = 1:5
    lambdau_h = sqrt(((sigma*Cla)./(16*F_h)).^2+((sigma*Cla*ftheta.*r)
        ./(8*F_h)))-((sigma*Cla)./(16*F_h));
    phi_h = lambdau_h./r; %Induced flow angle
    f_h = (N/2)*((1-r)./(r.*phi_h));
    F_h = (2/pi)*acos(exp(-f_h));
end
% Lower Rotor
Ac = pi*.707^2;
% r 1 - 15
Acen = pi*r(1:15).^2;
Fcen_h = F_h(1:15);
rcen = r(1:15);
lcenu_h = lambdau_h(1:15);
%thetacen = theta(1:15);

```

```

lambdalc_h = sqrt(((sigma*Cla)./(16*Fcen_h) - ((Acen/Ac).*lcenu_h)
    /(2)).^2 + (sigma*Cla.*ftheta.*rcen)./(8*Fcen_h)) - ((sigma*Cla)
    ./(16*Fcen_h) - ((Acen/Ac).*lcenu_h)/(2));
phicen_h = lambdalc_h./rcen;
fcen_h = (N/2)*((1-rcen)./(rcen.*phicen_h));
Fcen_h = (2/pi)*acos(exp(-fcen_h));
% r = 16 - 20;
Aout = pi*r(16:end).^2;
Fout_h = F_h(16:end);
rout = r(16:end);
loutu_h = lambdau_h(16:end);
%thetaout = theta(16:end);
lambdalo_h = sqrt(((sigma*Cla)./(16*Fout_h)).^2 + ((sigma*Cla*
    ftheta.*rout)./(8*Fout_h)) - ((sigma*Cla)./(16*Fout_h)));
%% Finding Ct
intup_h = lambdau_h.^2.*r;
Ctup_h = sum(intup_h(intup_h>0)*.05);
intlowcen_h = lambdalc_h.^2.*rcen;
Ctlowcen_h = sum(intlowcen_h(intlowcen_h>0)*.05);
intlowout_h = lambdalo_h.^2.*rout;
Ctlowout_h = sum(intlowout_h(intlowout_h>0)*.05);
Ct_h = 4*(Ctup_h+Ctlowcen_h+Ctlowout_h);
%finding Cp
inpup_h = intup_h.*lambdau_h;
Cpup_h = sum(inpup_h(inpup_h>0*.05));
inplowcen_h = intlowcen_h.*lambdalc_h;
Cplowcen_h = sum(inplowcen_h(inplowcen_h>0)*.05);
inplowout_h = intlowout_h.*lambdalo_h;
Cplowout_h = sum(inplowout_h(inplowout_h>0)*.05);
Cp_h = 4*(Cpup_h+Cplowcen_h+Cplowout_h);

```

```

Thrust_h = Ct_h*rho*A*Omega^2*R^2;
Power_h = Cp_h*rho*A*Omega^3*R^3;

fprintf('The Thrust produced for climb is %.01f N\n',Thrust)
fprintf('The Thrust produced for hover is %.01f N\n',Thrust_h)
fprintf('The Power produced during climb is %.01f W\n',Power)
fprintf('The Power produced during hover is %.01f W\n',Power_h)
%% Power Calculations
%%Equation
%%We are assuming values of k and kint based on research papers
Thov = Thrust_h;
P = (kint*k*(2*Thov)^(3/2))/sqrt(2*rho*A) + rho*A*(Omega*R)^3*((
    sigma*cdo)/4);
BR = 0:.1:4;
Bomega = Vtip./BR;
Bsigma = (N*c)./(pi*BR);
BA = pi*BR.^2;
BP = (kint*k*(2*Thov)^(3/2))./sqrt(2*rho*BA) + rho*BA.*(Bomega.*BR
    ).^3.*((Bsigma*cdo)/4);
fprintf('The Power required for hover is %.01f W\n',P)
%% Reynolds number
% Mach Number along blade
rmach= 0:.01:R;
Mach = (Omega*rmach)/a;
Re = (rho*Vtip*c)/mu;
Rex = (rho*Omega*rmach*c)/mu;
fprintf('The Reynolds number during hover is %.01f\n',Re)
%% RPM
RPM = (Vtip*60)/(pi*2*R);

```

```

fprintf('The required RPM for hover is %.01f\n',RPM)
%% Torque
Q = Power/Omega;
Q_h = Power_h/Omega;
fprintf('The required Torque for climb is %.01f Nm\n',Q)
fprintf('The required Torque for hover is %.01f Nm\n',Q_h)
%% Plots
%Lambda Upper
plot(r,lambdau,'k-')
%Lambda Lower Center
hold on
plot(rcen,lambdalc,'b-')
%Lambda Lower Outer
hold on
plot(rout,lambdalo,'r-')
xlabel('Radial station y/r','fontsize',12)
ylabel('Non-dimensionalized velocity (V/OmegaR)','fontsize',12)
title('Non-dimensionalized velocity as a function of radius for
      upper and lower props','fontsize',12)
legend('Upper Prop','Vena Contracta Lower Prop','Outer Lower Prop',
      , 'Location','SouthEast')
%Reynolds Number and Mach Number
figure
[hAx,hLine1,hLine2]=plotyy(rmach,Rex,rmach,Mach);
xlabel('Radius (m)','fontsize',12)
ylabel(hAx(1),'Reynold''s Number','fontsize',12) % left y-axis
ylabel(hAx(2),'Mach Number','fontsize',12) % right y-axis
title('Reynolds Number and Mach Number as a function of Radius
      along the blade','fontsize',11)
%Power as a function of radius

```

```
figure
plot(BR,BP)
xlabel('Radius(m)', 'fontsize',12)
ylabel('Power (W)', 'fontsize',12)
title('Hover Power required as a function of total Radius', '
      fontsize',12)
axis([0 3 0 4000])
```

References

- [1] A. Datta, *The Martian Autonomous Rotary-wing Vehicle (MARV)*, Tech. Rep., University of Maryland, College Park, Md, USA, 2000.
- [2] Leishman, J. G. and Ananthan, S., "Aerodynamic Optimization of a Coaxial Proprotor," 62nd Annual National Forum of the American Helicopter Society, Phoenix, AZ, May 9-11, 2006.
- [3] Young, L., Gulick, V., Briggs, G.A., "Rotorcraft as Mars Scouts". Presented at the 2002 IEEE Aerospace Conference, Big Sky, MT, March 9-16, 2002.
- [4] Rudin, Konrad, "Rotorcraft: Lecture 1, Introduction. Unmanned Aircraft Design, Modeling and Control, ETH, Swiss Federal Institute of Technology Zurich, 2011.
- [5] Seddon, J., *Basic Helicopter Aerodynamics*. AIAA Inc., Washington DC 1990